

Nonparametric maximum likelihood estimation under a likelihood ratio order

Ted Westling^{1,2}

Kevin J. Downes^{2,3,4}

Dylan S. Small^{1,5}

¹Center for Causal Inference, Perelman School of Medicine, University of Pennsylvania

²Center for Pediatric Clinical Effectiveness, Children’s Hospital of Philadelphia

³Division of Infectious Diseases, Children’s Hospital of Philadelphia

⁴Department of Pediatrics, Perelman School of Medicine, University of Pennsylvania

⁵Department of Statistics, The Wharton School, University of Pennsylvania

Abstract

Comparison of two univariate distributions based on independent samples from them is a fundamental problem in statistics, with applications in a wide variety of scientific disciplines. In many situations, we might hypothesize that the two distributions are stochastically ordered, meaning intuitively that samples from one distribution tend to be larger than those from the other. One type of stochastic order that arises in economics, biomedicine, and elsewhere is the likelihood ratio order, also known as the density ratio order, in which the ratio of the density functions of the two distributions is monotone non-decreasing. In this article, we derive and study the nonparametric maximum likelihood estimator of the individual distributions and the ratio of their densities under the likelihood ratio order. Our work applies to discrete distributions, continuous distributions, and mixed continuous-discrete distributions. We demonstrate convergence in distribution of the estimator in certain cases, and we illustrate our results using numerical experiments and an analysis of a biomarker for predicting bacterial infection in children with systemic inflammatory response syndrome.

1 Introduction

Estimation of the ratio of two density functions using independent samples from the densities is an important problem in a variety of fields. In many contexts, it may be known that this ratio is non-decreasing. In this article, we derive and study the nonparametric maximum likelihood estimator of the individual distributions as well as the ratio of their densities under the assumption that the density ratio is non-decreasing.

Comparing the distributions of two independent samples is a fundamental problem in statistics. Suppose that X_1, \dots, X_{n_1} and Y_1, \dots, Y_{n_2} are independent real-valued samples with distribution functions F_0 and G_0 , respectively. In many situations, we might hypothesize that F_0 and G_0 are *stochastically ordered*, meaning intuitively that samples from F_0 tend to be larger than those

from G_0 . A particular type of stochastic order that arises in many applications is the *likelihood ratio order*. We say that G_0 and F_0 satisfy a likelihood ratio order if the density ratio f_0/g_0 is monotone non-decreasing over the support \mathcal{G}_0 of G_0 , where $f_0 := dF_0/d\mu$ and $g_0 := dG_0/d\mu$ for some dominating measure μ . For this reason, the likelihood ratio order is also called a *density ratio order*.

A likelihood ratio order can arise for a variety of scientific reasons. For example, Dykstra et al. (1995) and Yu et al. (2017) considered its application to biomedical problems, while Beare and Moon (2015) and Roosen and Hennessy (2004) discussed numerous examples of its use in economics, business, and finance. Statistically, the likelihood ratio order assumption is a useful nonparametric generalization of many parametric and semiparametric models. For instance, monotone transformations of location families of log-concave densities satisfy a likelihood ratio order: if $F_0 = H_{\theta_1} \circ K$ and $G_0 = H_{\theta_2} \circ K$, where $H_\theta(x) := H(x - \theta)$, H is the distribution function corresponding to a log-concave density, $\theta_1 \geq \theta_2$, and K is non-decreasing, then f_0/g_0 is non-decreasing. As another example, if F_0 is any monotone exponential tilt of G_0 , meaning $f_0(x) = e^{h(x)}g_0(x)$ for a monotone function h , then $f_0/g_0 = e^h$ is clearly also monotone.

In this article, we address nonparametric estimation under the likelihood ratio order. We are especially interested in estimation and inference for the density ratio function f_0/g_0 . In the biomedical sciences and elsewhere, the ratio of two density functions is an object of interest for describing the relative likelihood of a binary status indicator conditional on a covariate. If D is a binary random variable, Z is a scalar random variable, $F_0(z) = P_0(Z \leq z \mid D = 1)$, $G_0(z) = P(Z \leq z \mid D = 0)$, and $H_0(z) := P(Z \leq z)$, then the density ratio equals

$$\frac{f_0(z)}{g_0(z)} = \frac{[dF_0/dH_0](z)}{[dG_0/dH_0](z)} = \frac{P(D = 1 \mid Z = z)/P(D = 1)}{P(D = 0 \mid Z = z)/P(D = 0)}. \quad (1)$$

Therefore, the density ratio in this context may be interpreted as the relative odds of $D = 1$ given $Z = z$ to the overall odds of $D = 1$. Since the transformation $x \mapsto x/(1 - x)$ is strictly increasing, monotonicity of the density ratio is equivalent to monotonicity of the conditional probability $P(D = 1 \mid Z = z)$ in z .

One specific situation in which the representation given in (1) is of scientific interest is biomarker evaluation. Over the past few decades, there has been a rapid increase in the development of assays

to measure the concentration of various biochemicals in human sera, with the goal of predicting clinical disease status. In these contexts, D represents disease status and Z represents the value of a biomarker. Equation (1) implies that the ratio of the densities of biomarker values among infected patients to the same among uninfected patients can be interpreted as the odds ratio of infection given biomarker level relative to overall odds of infection. Monotonicity of the density ratio corresponds to the assumption that the conditional probability of infection given biomarker level increases with biomarker level, which is a reasonable assumption if the biomarker is actually predictive of disease.

A second example of situations in which a density ratio may be of scientific interest is experiments with continuous exposures and binary outcomes. Suppose now that Z represents a continuous exposure, and $D(z)$ represents the potential outcome under assignment to exposure $Z = z$. The causal odds of Z on the potential outcome $D(z)$ is then defined as $z \mapsto P(D(z) = 1)/P(D(z) = 0)$. If $D(z)$ is independent of the observed exposure Z , as is true in randomized experiments, and additional causal conditions hold, then the causal odds equals $P(D = 1 | Z = z)/P(D = 0 | Z = z)$, where $D := D(Z)$ is the observed outcome. If f_0 is the density of Z in units with $D = 1$ and g_0 is the density of Z in units with $D = 0$, then this further equals $[f_0(z)/g_0(z)][P(D = 1)/P(D = 0)]$. In some contexts, it may be known that $P(D(z) = 1)$ is monotone in the exposure z , in which case the density ratio $f_0(z)/g_0(z)$ is as well.

In this article, we derive the nonparametric maximum likelihood estimators of F_0 , G_0 , and $\theta_0 = f_0/g_0$ under the likelihood ratio order restriction and derive certain asymptotic properties of these estimators, including consistency and convergence in distribution. In particular, we connect estimation of θ_0 to the classical isotonic regression problem with a binary outcome, which both simplifies the derivation of large-sample results and suggests that existing inference methods for the isotonic regression problem can be used to perform inference for θ_0 as well. Our results generalize those of Dykstra et al. (1995), who derived the maximum likelihood estimator of F_0 and G_0 under a likelihood ratio order in the special case where F_0 and G_0 are discrete distributions. We illustrate our results using numerical experiments and an analysis of a biomarker for predicting bacterial infection in children with systemic inflammatory response syndrome.

Recently, Yu et al. (2017) considered estimation of a monotone density ratio function by maximizing a smoothed likelihood function, and demonstrated certain asymptotic properties of their

estimator. Yu et al. (2017) considered maximizing a smoothed likelihood rather than maximizing the likelihood directly because they claimed a maximum likelihood estimator does not exist. However, we show that, using a definition of the likelihood ratio ordered model based on convexity of the ordinal dominance curve, a well-defined nonparametric maximum likelihood estimator does exist. Furthermore, unlike the smoothed estimator, the derivation of the maximum likelihood estimator does not rely on the existence of Lebesgue density functions, and works equally well when F_0 and G_0 are discrete or have discrete components.

As is common in the monotonicity-constrained literature, there are certain tradeoffs to maximizing the smoothed and non-smoothed likelihood functions. In particular, the non-smoothed estimator converges pointwise at the $n^{-1/3}$ rate, while the smoothed estimator converges at the faster $n^{-2/5}$ rate, albeit under stronger smoothness assumptions. While Yu et al. (2017) did not propose a method for conducting inference, smoothed estimators typically possess an asymptotic bias that complicates the task of performing valid inference. In contrast, we demonstrate that the non-smoothed estimator converges pointwise to a mean zero limit distribution, which we use to construct asymptotically valid inference. An additional benefit of the non-smoothed estimator is that it does not depend on a bandwidth or any other tuning parameter. Finally, while the smoothed estimator relies on absolute continuity of F_0 and G_0 with respect to Lebesgue measure, we demonstrate that the maximum likelihood estimator does not, and indeed performs well even with distributions with mixed continuous and discrete parts.

Additional relevant references include: Lehmann and Rojo (1992) and Shaked and Shanthikumar (2007), which contain more examples and details regarding stochastic orders, Carolan and Tebbs (2005) and Beare and Moon (2015), which studied tests of the likelihood ratio order, and Rojo and Samaniego (1991), Rojo and Samaniego (1993), Mukerjee (1996), Arcones and Samaniego (2000), Davidov and Herman (2012), and Tang et al. (2017), which considered testing and estimation under other stochastic orders.

2 Likelihood ratio orders

We observe two independent real-valued samples X_1, \dots, X_{n_1} and Y_1, \dots, Y_{n_2} with distribution functions F_0 and G_0 , respectively. We define \mathcal{F}_0 as the support of F_0 and \mathcal{G}_0 as the support of G_0 .

We denote $n := n_1 + n_2$, and by F_n and G_n the empirical distribution functions of X_1, \dots, X_{n_1} and Y_1, \dots, Y_{n_2} , respectively. We define $x_1 < \dots < x_{m_1}$ as the unique values of X_1, \dots, X_{n_1} , $y_1 < \dots < y_{m_2}$ as the unique values of Y_1, \dots, Y_{n_2} , and $z_1 < z_2 < \dots < z_m$ as the unique values of $(X_1, \dots, X_{n_1}, Y_1, \dots, Y_{n_2})$. Throughout, we assume that it is not the case that $y_{m_2} \leq x_1$ – i.e. we assume that $X_i < Y_j$ for some i, j . We also assume that $\pi_n := n_1/n \xrightarrow{P} \pi_0 \in (0, 1)$ as $n \rightarrow \infty$.

We let \mathcal{D} be the space of distribution functions on \mathbb{R} ; i.e. all non-decreasing, càdlàg functions H such that $\lim_{x \rightarrow -\infty} H(x) = 0$ and $\lim_{x \rightarrow \infty} H(x) = 1$. For any nondecreasing function $h : \mathbb{R} \rightarrow \mathbb{R}$, we define its *generalized-inverse* h^- pointwise as $h^-(u) := \inf\{x : h(x) \geq u\}$. When $h \in \mathcal{D}$, h^- is called the *quantile function* of h . For any interval $I \subseteq \mathbb{R}$ and any function $h : I \rightarrow \mathbb{R}$, we define the *greatest convex minorant* (GCM) of h on I , denoted $\text{GCM}_I(h) : I \rightarrow \overline{\mathbb{R}}$, for $\overline{\mathbb{R}}$ the extended real line, as the pointwise supremum of all convex functions on I bounded above by h . The least concave majorant operator is defined analogously. We say a function H is *convex over a set* $\mathcal{S} \subseteq \mathbb{R}$ if for every $x, y \in \mathcal{S}$ and $\lambda \in [0, 1]$ such that $\lambda x + (1 - \lambda)y \in \mathcal{S}$, $H(\lambda x + (1 - \lambda)y) \leq \lambda H(x) + (1 - \lambda)H(y)$. We also define ∂_- as the left derivative operator for a left differentiable function.

The unrestricted nonparametric model for the pair (F, G) of distribution functions of the observed data is $\mathcal{M}_{NP} := \mathcal{D}^2$. As mentioned in the introduction, the likelihood ratio order can be defined as the ratio of the density functions f_0 and g_0 of F_0 and G_0 , with respect to some dominating measure μ , being non-decreasing. By varying the dominating measure μ , both discrete and continuous distributions can be handled this way. However, as noted by Yu et al. (2017), this definition does not lend itself to the derivation of a maximum likelihood estimator, since the likelihood defined through the densities can be made arbitrarily large. Instead, other authors have defined the likelihood ratio order as convexity of the *ordinal dominance curve*, defined as $t \mapsto R_{F,G}(t) := F \circ G^-(t)$ for $t \in [0, 1]$ (Bamber, 1975; Hsieh and Turnbull, 1996). Lehmann and Rojo (1992) demonstrated the equivalence of this definition to that using the density functions in the special case that F and G are strictly increasing and continuous on their supports, which were assumed to be intervals. In Theorem 1 below, we generalize this result.

Theorem 1. *If $F \ll G$ and $\nu := dF/dG$ is continuous on the support \mathcal{G} of G , then (1) $R_{F,G}$ is convex on $\text{Im}(G)$ if and only if ν is non-decreasing on \mathcal{G} , and (2) if ν is non-decreasing on \mathcal{G} then $\nu(x) = \partial_- \text{GCM}_{[0,1]}(R_{F,G}) \circ G(x)$ for all $x \in \mathcal{G}$.*

To our knowledge, Theorem 1 is the most general result to-date connecting the likelihood ratio ordered model, defined via monotonicity of the density ratio function, to convexity of the ordinal dominance curve. Theorem 1 then justifies the following definitions. We say $(F, G) \in \mathcal{M}_{NP}$ satisfy a likelihood ratio order, and write $G \leq_{LR} F$ if $R_{F,G}$ is convex on $\text{Im}(G)$. We then define the likelihood ratio ordered model \mathcal{M}_{LR} as all $(F, G) \in \mathcal{M}_{NP}$ such that $G \leq_{LR} F$. For any $(F, G) \in \mathcal{M}_{NP}$, we further define $\theta : \mathcal{M}_{NP} \rightarrow \Theta$ as $\theta_{F,G} := \partial\text{-GCM}_{[0,1]}(R_{F,G}) \circ G$, where Θ is defined as the set of non-negative, non-decreasing functions on \mathbb{R} . By Theorem 1, for all $(F, G) \in \mathcal{M}_{LR}$ such that $F \ll G$ and dF/dG is continuous on \mathcal{G} , $\theta_{F,G} = dF/dG$ on \mathcal{G} . We define $\theta_0 := \theta_{F_0, G_0}$.

In the context of the likelihood ratio order, many existing works either assume that F_0 and G_0 are discrete (e.g. Dykstra et al., 1995) or that F_0 and G_0 are continuous (e.g. Lehmann and Rojo, 1992; Yu et al., 2017). In the discrete setting, if F_0 and G_0 are discrete distributions with common support and mass functions ΔF_0 and ΔG_0 such that $(F_0, G_0) \in \mathcal{M}_{LR}$, then $\theta_0 = \Delta F_0 / \Delta G_0$ on \mathcal{G}_0 . Alternatively, if F_0 and G_0 both possess Lebesgue density functions f_0 and g_0 and $(F_0, G_0) \in \mathcal{M}_{LR}$, then $\theta_0 = f_0 / g_0$ on \mathcal{G}_0 . However, for the purpose of deriving a maximum likelihood estimator, we will demonstrate that these two cases do not need to be treated separately. Furthermore, in some applied settings, F_0 and G_0 are neither discrete nor continuous, but rather a mixture of discrete and continuous components, and we will derive results that apply in these situations as well. For instance, exposures that are bounded below may have positive mass at their lower boundary, and be continuous thereafter. Many biomarkers exhibit this property. Similarly, some measurements are “clumpy”, exhibiting positive mass at integers or other “round” numbers due to the measurement process, but also possessing positive Lebesgue density between such points. In all cases, θ_0 has a meaningful interpretation as the ratio of the conditional odds of a sample being from the distribution F_0 to the unconditional odds of a sample being from F_0 .

3 Estimation under a likelihood ratio order

3.1 Maximum likelihood estimator

The pair (F_0, G_0) determines the joint distribution of the observed data. The nonparametric maximum likelihood estimator of (F_0, G_0) , i.e. in the model \mathcal{M}_{NP} , is (F_n, G_n) for F_n the empirical distribution function of X_1, \dots, X_{n_1} , and G_n the same of Y_1, \dots, Y_{n_2} . This suggests taking as an

estimator of θ_0 the plug-in estimator $\theta_n := \theta_{F_n, G_n} = \partial_- \text{GCM}_{[0,1]}(F_n \circ G_n^-) \circ G_n$. The function $F_n \circ G_n^-$ is known as the *empirical ordinal dominance curve*, and its properties were studied by Hsieh and Turnbull (1996).

In this section, we demonstrate, amongst other results, that θ_n is the maximum likelihood estimator of θ_0 in the likelihood ratio ordered model \mathcal{M}_{LR} . Defining the nonparametric likelihood of the observed data as

$$L_n(F, G) := \left\{ \prod_{i=1}^{n_1} [F(X_i) - F(X_i-)] \right\} \left\{ \prod_{j=1}^{n_2} [G(Y_j) - G(Y_j-)] \right\},$$

a maximum likelihood estimator of (F_0, G_0) in \mathcal{M}_{LR} is defined as $(F_n^*, G_n^*) \in \arg\max_{(F, G) \in \mathcal{M}_{LR}} L_n(F, G)$, and a maximum likelihood estimator of θ_0 is defined as $\theta_n^* := \theta_{F_n^*, G_n^*}$.

We define $H_n(z) := \pi_n F_n(z) + (1 - \pi_n) G_n(z)$ as the empirical distribution of the combined sample $X_1, \dots, X_{n_1}, Y_1, \dots, Y_{n_2}$, and $h_k := H_n(y_k)$ for $k = 1, \dots, m_2$. Our first result characterizes (F_n^*, G_n^*) .

Theorem 2. *Let A_k^* be the value at h_k of the GCM over $[0, h_{m_2}]$ of $\{(h_k, F_n(y_k)) : k = 0, \dots, m_2\}$ and B_k^* be the value at h_k of the LCM over $[0, h_{m_2}]$ of $\{(h_k, G_n(y_k)) : k = 0, \dots, m_2\}$. Then G_n^* is a right-continuous step function with jumps at y_1, \dots, y_{m_2} with $G_n^*(y_k) = B_k^*$ and F_n^* is given by a right-continuous step function with jumps at z_1, \dots, z_m , where $F_n^*(y_k) = A_k^*$, and for any x_i such that $y_{j-1} < x_i \leq y_j$, where $y_0 := -\infty$, the mass of F_n^* at x_i is given by*

$$F_n^*(x_i) - F_n^*(x_i-) = [F_n^*(y_j) - F_n^*(y_{j-1})] \frac{F_n(x_i) - F_n(x_i-)}{F_n(y_j) - F_n(y_{j-1})}.$$

For any x_i such that $y_{m_2} < x_i$, the mass of F_n^* at x_i is given by

$$F_n^*(x_i) - F_n^*(x_i-) = [1 - F_n^*(y_{m_2})] \frac{F_n(x_i) - F_n(x_i-)}{1 - F_n(y_{m_2})}.$$

We also note that $F_n^*(y_k) = \text{GCM}_{[0, h_{m_2}]}(F_n \circ H_n^-)(H_n(y_k))$ and $G_n^*(y_k) = \text{LCM}_{[0, h_{m_2}]}(G_n \circ H_n^-)(H_n(y_k))$.

A proof of Theorem 2, and proofs of all other theorems, are provided in Supplementary Material. We note that if there are j such that no $x_i \in (y_j, y_{j+1}]$ but $F_n^*(y_j) > F_n^*(y_{j-1})$, then there are infinitely many maximizers F_n^* because any F_n^* that assigns mass $F_n^*(y_j) - F_n^*(y_{j-1})$ to the interval

$(y_j, y_{j+1}]$ yields the same likelihood and satisfies the constraints. In these cases, for the sake of uniqueness, we will put mass $F_n^*(y_j) - F_n^*(y_{j-1})$ at the point y_{j+1} . Theorem 2 agrees with the main result of Dykstra et al. (1995) in the special case that F_0 and G_0 are finite discrete distributions.

Theorem 2 implies the following result characterizing θ_n^* .

Corollary 1. *The points $\{(G_n^*(y_k), F_n^*(y_k)) : k = 1, \dots, m_2\}$ lie on the GCM over $[0, 1]$ of the empirical ordinal dominance curve $\{(G_n(y_j), F_n(y_j)) : k = 0, \dots, m_2\}$, where $y_0 := -\infty$. Specifically, if $\{(h_{j_k}, F_n(y_{j_k})) : k = 0, \dots, K\}$ are the vertices of the GCM of $\{(h_k, F_n(y_k)) : k = 0, \dots, m_2\}$, then $(G_n(y_{j_k}), F_n(y_{j_k})) : k = 0, \dots, K\}$ are the vertices of the GCM of the empirical ordinal dominance curve. Therefore, $\theta_n^* := \theta_{F_n^*, G_n^*}$ is equal to $\theta_n := \theta_{F_n, G_n}$.*

We illustrate the use of Theorem 2 and Corollary 1 using hypothetical data. Suppose that $(Y_1, \dots, Y_6) = (0, 0, 1, 3, 3, 6)$ and $(X_1, \dots, X_4) = (-1, 2, 3, 3)$. We first derive F_n^* . The points $\{(H_n(y_k), F_n(y_k)) : k = 0, \dots, m_2\}$ are given by $\{(0, 0), (0.3, 0.25), (0.4, 0.25), (0.9, 1), (1, 1)\}$, and its GCM is given by $\{(0, 0), (0.3, 3/16), (0.4, 1/4), (0.9, 7/8), (1, 1)\}$. This is displayed in the upper left panel of Figure 1. The values of the GCM imply that $F_n^*(0) = 3/16$, $F_n^*(1) = 1/4$, $F_n^*(3) = 7/8$, and $F_n^*(6) = 1$. We then have that $F_n^*(-1) = F_n^*(-\infty) + [F_n^*(0) - F_n^*(-\infty)] \frac{F_n(-1) - F_n(-\infty)}{F_n(0) - F_n(-\infty)} = [3/16] \frac{1/4}{1/4} = 3/16$ and $F_n^*(2) = F_n^*(1) + [F_n^*(3) - F_n^*(1)] \frac{F_n(2) - F_n(1)}{F_n(3) - F_n(1)} = 1/4 + [5/8] \frac{1/4}{3/4} = 11/24$. The estimators F_n and F_n^* are compared in the bottom left panel of Figure 1.

We next derive G_n^* . The points $\{(H_n(y_k), G_n(y_k)) : k = 0, \dots, m_2\}$ are given by $\{(0, 0), (0.3, 1/3), (0.4, 1/2), (0.9, 5/6), (1, 1)\}$, and its LCM is given by $\{(0, 0), (0.3, 3/8), (0.4, 1/2), (0.9, 11/12), (1, 1)\}$. This is displayed in the center left panel of Figure 1. The values of the LCM imply that $G_n^*(0) = 3/8$, $G_n^*(1) = 1/2$, $G_n^*(3) = 11/12$, and $G_n^*(6) = 1$. The estimators G_n and G_n^* are compared in the bottom left panel of Figure 1.

Finally, we derive θ_n^* . The empirical ordinal dominance curve is given by the points $\{(0, 0), (1/3, 1/4), (1/2, 1/4), (5/6, 1), (1, 1)\}$, and the vertices of its GCM are given by $\{(0, 0), (1/2, 1/4), (1, 1)\}$. This is displayed in the bottom left panel of Figure 1. The left-hand slopes of the GCM are $1/2$ on the interval $(0, 1/2]$ and $3/2$ on the interval $(1/2, 1]$, which implies that $\theta_n^*(z) = 1/2$ for $z \in (-\infty, 1]$ and $\theta_n^*(z) = 3/2$ for $z \in (1, \infty)$. This is displayed in the bottom right panel of Figure 1.

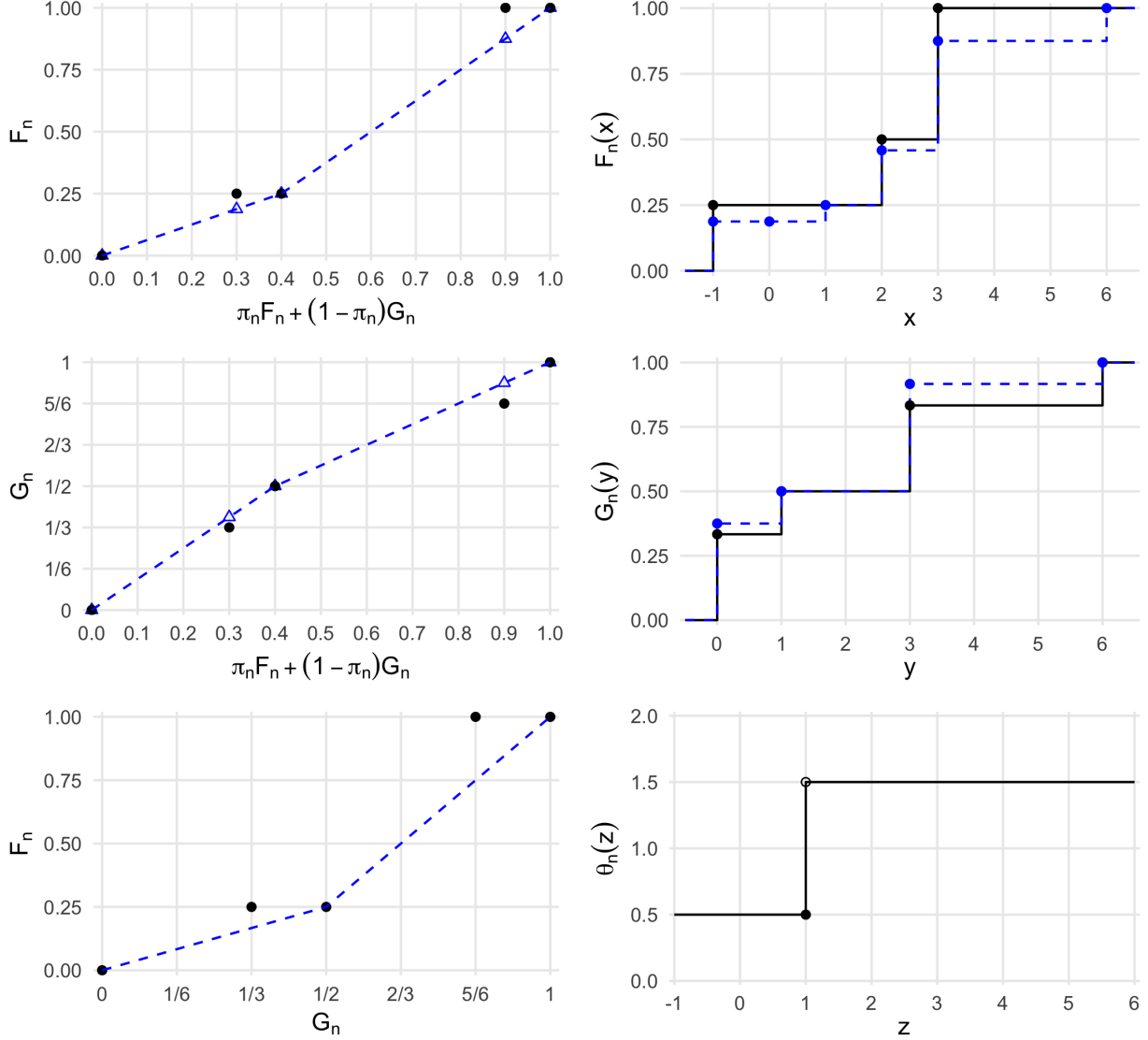


Figure 1: Example of the process of constructing the maximum likelihood estimator for $(Y_1, \dots, Y_6) = (0, 0, 1, 3, 3, 6)$ and $(X_1, \dots, X_4) = (-1, 2, 3, 3)$. The graph of F_n versus $\pi_n F_n + (1 - \pi_n) G_n$ evaluated at z_1, \dots, z_m and its GCM are shown in the upper left. The resulting MLE F_n^* and F_n are shown in the upper right, and the graph of G_n versus $\pi_n F_n + (1 - \pi_n) G_n$ evaluated at z_1, \dots, z_m and its LCM are shown in the center left, and the resulting MLE G_n^* and G_n are shown in the middle right. The ODC diagram of F_n versus G_n and its GCM are shown in the bottom left, and the resulting MLE θ_n^* is shown in the bottom right.

3.2 Representation as a transformation of isotonic regression

The form of θ_n^* can be derived in a simpler way without relying on Theorem 2 by reframing the problem as a transformation of an isotonic regression with a binary outcome. We let D_1, \dots, D_n be independent Bernoulli random variables with common probability π_0 and such that $n_1 = \sum_{i=1}^n D_i$.

Letting j_1, \dots, j_{n_1} be the indices such that $D_{j_i} = 1$ for each i , we then define $Z_{j_i} := X_i$ for each $i = 1, \dots, n_1$. Similarly, letting k_1, \dots, k_{n_2} be the indices such that $D_{k_i} = 0$ for each i , we define $Z_{k_i} := Y_i$ for each $i = 1, \dots, n_2$. Defining the data unit $\mathbf{O}_i := (Z_i, D_i)$, observing the independent samples X_1, \dots, X_{n_1} from F_0 and Y_1, \dots, Y_{n_2} from G_0 is then equivalent to observing independent observations $\mathbf{O}_1, \dots, \mathbf{O}_n$ from P_0 , where P_0 satisfies

$$P_0(Z \leq z, D = d) = d\pi_0 F_0(z) + (1 - d)(1 - \pi_0)G_0(z) .$$

Thus, Z_1, \dots, Z_n represent the pooled values of $X_1, \dots, X_{n_1}, Y_1, \dots, Y_{n_2}$, and each D_i represents an indicator that Z_i corresponds to a sample from F_0 . Furthermore, $F_0(z) = P_0(Z \leq z \mid D = 1)$, $G_0(z) = P_0(Z \leq z \mid D = 0)$, and $\pi_0 := P_0(D = 1)$. Estimating θ_0 given the independent samples X_1, \dots, X_{n_1} and Y_1, \dots, Y_{n_2} is therefore equivalent to estimating θ_0 given independent observations $\mathbf{O}_1, \dots, \mathbf{O}_n$ from P_0 , where $n_1 := \sum_{i=1}^n D_i$.

The benefit to the above reframing of the problem is that θ_0 , F_0 , and G_0 can then be written as transformations of P_0 . First, we have that $\theta_0(z) = T(\mu_0(z))/T(\pi_0)$, where $\mu_0(z) := P_0(D = 1 \mid Z = z)$ and $T : [0, 1) \rightarrow \mathbb{R}^+$ is the odds transformation, defined as $T(\mu) := \mu/(1 - \mu)$. Since T is strictly increasing, θ_0 is monotone if and only if μ_0 is. Since the maximum likelihood estimator of μ_0 under the assumption that μ_0 is non-decreasing is given by the isotonic regression μ_n^* of D_1, \dots, D_n on Z_1, \dots, Z_n , and the maximum likelihood estimator of π_0 is given by π_n , the maximum likelihood estimator of $\theta_0(z)$ is then given by $T(\mu_n^*(z))/T(\pi_n)$. Similarly, $F_0(z) = \pi_0^{-1} \int_{-\infty}^z \mu_0(u) dH_0(u)$ and $G_0(z) = (1 - \pi_0)^{-1} \int_{-\infty}^z [1 - \mu_0(u)] dH_0(u)$. Since the maximum likelihood estimator of H_0 is given by the empirical distribution H_n of Z_1, \dots, Z_n , the maximum likelihood estimators of F_0 and G_0 are given by $\pi_n^{-1} \int_{-\infty}^z \mu_n^*(u) dH_n(u)$ and $(1 - \pi_n)^{-1} \int_{-\infty}^z [1 - \mu_n^*(u)] dH_n(u)$. It is straightforward to see that these forms of the maximum likelihood estimators are equivalent to the forms given above. In the next section, we will utilize this form of θ_n^* to derive its asymptotic properties and to construct asymptotic confidence intervals.

4 Asymptotic results

4.1 Discrete distributions

We first consider the situation where both F_0 and G_0 have finite support and θ_0 , which in this case corresponds to the ratio of the mass functions $\Delta F_0/\Delta G_0$, is strictly increasing on \mathcal{G}_0 . In this case, R_0 is strictly convex on $\text{Im}(\mathcal{G}_0)$, and with probability tending to one, the empirical ordinal dominance curve $F_n^* \circ G_n^-$ is also strictly convex. As a result, $\|F_n^* - F_n\|_\infty = o_P(n^{-1/2})$ and $\|G_n^* - G_n\|_\infty = o_P(n^{-1/2})$, where $\|\cdot\|_\infty$ denotes the supremum norm. Therefore, letting ΔF_n^* and ΔG_n^* be the mass functions corresponding to F_n^* and G_n^* , respectively, we have that $n^{1/2}[\Delta F_n^*(z) - \Delta F_0(z)]$ and $n^{1/2}[\Delta G_n^*(z) - \Delta G_0(z)]$ converge in distribution to independent normal distributions with mean 0 and variances $\pi_0^{-1}\Delta F_0(z)[1 - \Delta F_0(z)]$ and $(1 - \pi_0)^{-1}\Delta G_0(z)[1 - \Delta G_0(z)]$, respectively. A straightforward application of the delta-method then implies that $n^{1/2}[\theta_n^*(z) - \theta_0(z)]$ converges in distribution to a mean-zero normal with variance $\theta_0(z)[\pi_0\Delta F_0(z) + (1 - \pi_0)\Delta G_0(z) - \Delta F_0(z)\Delta G_0(z)]/[\pi_0(1 - \pi_0)\Delta G_0(z)^2]$.

4.2 Continuous distributions

Now we address the situation where F_0 and G_0 are both absolutely continuous on \mathcal{G}_0 and θ_0 , which now corresponds to the ratio f_0/g_0 of the density functions, is strictly increasing. We first consider the large-sample behavior of F_n^* and G_n^* . This study is aided by the work of Beare and Fang (2017), who demonstrated that the LCM operation is a directionally Hadamard differentiable mapping at any concave function. In particular, the Hadamard derivative at a concave R_0 is equal to the identity operator if and only if R_0 is strictly concave. The functional delta-method therefore implies that $\|F_n^* - F_n\|_\infty = o_P(n^{-1/2})$ and $\|G_n^* - G_n\|_\infty = o_P(n^{-1/2})$ since $R_0 = F_0 \circ G_0^-$ is strictly convex by assumption. When θ_0 has flat sections, so that R_0 has affine sections, the form of the Hadamard derivative provided by Beare and Fang (2017) can be used in conjunction with the chain rule to derive the weak limits of the processes $\{n^{1/2}[F_n^*(x) - F_0(x)] : x \in \mathbb{R}\}$ and $\{n^{1/2}[G_n^*(y) - G_0(y)] : y \in \mathbb{R}\}$. Since the Hadamard derivative of the GCM operation is weakly contractive, these limit processes are more concentrated than those of $\{n^{1/2}[F_n(x) - F_0(x)] : x \in \mathbb{R}\}$ and $\{n^{1/2}[G_n(y) - G_0(y)] : y \in \mathbb{R}\}$, which implies consistency at the rate $n^{-1/2}$ of F_n^* and G_n^* .

We now turn to large-sample results for θ_n at points z where both F_0 and G_0 possess Lebesgue

density functions f_0 and g_0 , respectively. First, consistency of μ_n^* implies consistency of θ_n^* .

Theorem 3 (Consistency). *If f_0 is continuous at x , g_0 is continuous at x , and $g_0(x) > 0$, then $\theta_n^*(x) \xrightarrow{P} \theta_0(x)$. If f_0 and g_0 are uniformly continuous on \mathcal{G}_0 , then $\sup_{x \in I} |\theta_n^*(x) - \theta_0(x)| \xrightarrow{P} 0$ for any strict sub-interval $I \subsetneq \mathcal{G}_0$.*

We recall that, at any z such that $h_0 = \pi_0 f_0 + (1 - \pi_0)g_0$ is positive and continuous in a neighborhood of z , $\mu_0(z) \in (0, 1)$, and μ_0 is continuously differentiable in a neighborhood of z , it holds that

$$n^{1/3} [\mu_n^*(z) - \mu_0(z)] \xrightarrow{d} \{4\mu_0'(z)\mu_0(z)[1 - \mu_0(z)]h_0(z)^{-1}\}^{1/3} W, \quad (2)$$

where W follows *Chernoff's distribution*, defined as the point of maximum of $Z(u) - u^2$ for Z a two-sided standard Brownian motion originating from zero. We can then use the delta-method to see that

$$n^{1/3} [\theta_n^*(z) - \theta_0(z)] \xrightarrow{d} T(\pi_0)T'(\mu_0) \{4\mu_0'(z)\mu_0(z)[1 - \mu_0(z)]h_0(z)^{-1}\}^{1/3} W.$$

The scale parameter in the above limit distribution is equal to $[4\kappa_0(z)\theta_0'(z)]^{1/3}$ for

$$\kappa_0(z) := \theta_0(z) \frac{\pi_0 f_0(z) + (1 - \pi_0)g_0(z)}{\pi_0(1 - \pi_0)g_0(z)^2}.$$

This yields the following result.

Theorem 4 (Pointwise convergence in distribution). *Suppose that, in a neighborhood of z , θ_0 is continuously differentiable with $\theta_0'(z) > 0$, and f_0 and g_0 are positive and continuous. Then*

$$n^{1/3} [\theta_n^*(z) - \theta_0(z)] \xrightarrow{d} [4\kappa_0(z)\theta_0'(z)]^{1/3} W.$$

Theorem 4 provides a means to construct asymptotically valid confidence intervals for $\theta_0(z)$ at any z such that $g_0(z) > 0$. Defining $\tau_n(z)$ as an estimator of $\tau_0(z) := \kappa_0(z)\theta_0'(z)$ and q_α the $1 - \alpha/2$ quantile of W , a $100(1 - \alpha)\%$ Wald-type confidence interval for $\theta_0(z)$ is given by

$$\left[\theta_n^*(z) - \{4\tau_n(z)/n\}^{1/3} q_{1-\alpha/2}, \theta_n^*(z) + \{4\tau_n(z)/n\}^{1/3} q_{1-\alpha/2} \right]. \quad (3)$$

If $\tau_n(z) \xrightarrow{P} \tau_0(z)$, then this interval has asymptotic coverage of $100(1 - \alpha)\%$. The quantiles of W were computed by Groeneboom and Wellner (2001), and in particular $q_{0.975} \approx 0.9982$.

In practice, we recommend an alternative method to constructing confidence intervals for $\theta_0(z)$. We recommend first constructing confidence intervals for $\mu_0(z)$ using either of two existing methods, then transforming these intervals into intervals for $\theta_0(z)$. Specifically, if $[\ell_n(z), u_n(z)]$ represents a $100(1 - \alpha)\%$ confidence interval for $\mu_0(z)$, then we take

$$[T(\ell_n(z))/T(\pi_n), T(u_n(z))/T(\pi_n)]$$

as a $100(1 - \alpha)\%$ confidence interval for $\theta_0(z)$. Two existing ways to construct $[\ell_n(z), u_n(z)]$ are Wald-type intervals with plug-in estimation of nuisance parameters and intervals based on likelihood ratio tests. The former intervals are analogous to the Wald-type interval (3), but based on the limit distribution for $n^{1/3}[\mu_n^*(z) - \mu_0(z)]$ given in (2). Alternatively, confidence intervals obtained by inverting likelihood ratio tests, proposed first by Banerjee and Wellner (2001) and studied further by, e.g. Banerjee (2007) and Groeneboom and Jongbloed (2015), can be formed based on the limiting distribution of twice the log of the ratio of the likelihoods of the maximum likelihood estimator and a suitably constrained maximum likelihood estimator. Since this limiting distribution is pivotal, meaning it does not depend on any unknown features of the true distribution, this approach does not require estimating any unknown nuisance parameters. We therefore expect this method to have better finite-sample properties than intervals based on plug-in estimation of nuisance parameters.

5 Numerical studies

In Supplementary Material, we present results of two simulation studies in the cases where F_0 and G_0 are fully discrete and fully continuous. In short, these studies confirm the validity of our large-sample theory and demonstrate that the maximum likelihood estimator and various proposed methods of conducting inference perform well in both cases. Here, we present the results of a numerical study illustrating the behavior of θ_n^* when F_0 and G_0 are mixed discrete-continuous distributions. We note that our asymptotic results did not address the behavior of θ_n^* at mass

points in mixed discrete-continuous distributions; to the best of our knowledge, no such results yet exist for monotone estimators. We use this numerical study to explore this important case.

We simulated Y as a mixed discrete-continuous random variable with probability $1/9$ each of being 0, 0.5 and 1, and probability $2/3$ of being from the uniform distribution on $[0, 1]$, and simulated X as a mixed discrete-continuous random variable with probabilities $1/18$, $1/9$, and $3/18$ of being 0, 0.5, and 1, respectively and probability $2/3$ of being from the density function $x \mapsto I_{[0,1]}(x)(0.5 + x)$. We then have that $\theta_0(x) = 0.5 + x$ for $x \in [0, 1]$. We set $\pi_0 := 0.4$. For each combined sample size $n \in \{500, 1K, 5K, 10K\}$, we simulated 1000 datasets, and in each dataset we computed the maximum likelihood estimator, the maximum smoothed likelihood estimator of Yu et al. (2017), and the non-monotone estimator based on kernel density estimates for each $z \in \{0, 0.05, \dots, 0.95, 1\}$. We constructed confidence intervals at each z using the transformed plug-in and likelihood ratio-based methods described in Section 4.2.

In addition to the properties of the estimators listed above, we also investigated the properties of the general sample-splitting procedure proposed by Banerjee et al. (2019). Given a generic monotone estimator γ_n of a monotone function γ_0 such that $n^{1/3}[\gamma_n(z) - \gamma_0(z)] \xrightarrow{d} G$ for G a mean-zero distribution with finite variance, Banerjee et al. (2019) proposed randomly splitting the sample into m subsets of roughly equal size, computing monotone estimates $\gamma_{n,1}, \dots, \gamma_{n,m}$ in each subset, then defining $\bar{\gamma}_{n,m}(z) := \frac{1}{m} \sum_{j=1}^m \gamma_{n,j}(z)$. They demonstrated that if $m > 1$ is fixed, then under mild conditions $\bar{\gamma}_{n,m}(z)$ has strictly better asymptotic mean squared error than $\gamma_n(z)$, and that for moderate m ,

$$\left[\bar{\gamma}_{n,m}(z) - \frac{\sigma_{n,m}(z)}{\sqrt{mn}^{1/3}} t_{1-\alpha/2, m-1}, \bar{\gamma}_{n,m}(z) + \frac{\sigma_{n,m}(z)}{\sqrt{mn}^{1/3}} t_{1-\alpha/2, m-1} \right] \quad (4)$$

forms an asymptotic $100(1-\alpha)\%$ confidence interval for $\gamma_0(z)$, where $\sigma_{n,m}^2(z) := \frac{1}{m-1} \sum_{j=1}^m [\gamma_{n,j}(z) - \bar{\gamma}_{n,m}(z)]^2$ and $t_{1-\alpha/2, m-1}$ is the $100(1 - \alpha/2)$ quantile of the t -distribution with $m - 1$ degrees of freedom. Therefore, $\bar{\gamma}_{n,m}(z)$ is preferable to $\gamma_n(z)$ for two reasons: it has better asymptotic mean squared error, and asymptotically valid pointwise confidence intervals for γ_0 based on $\bar{\gamma}_{n,m}$ can be formed without estimating any nuisance parameters. They also studied the asymptotic properties of $\bar{\gamma}_{n,m_n}(z)$ when m_n grows with n . In our simulation study, we considered the estimator $\bar{\theta}_{n,m}$ defined as $\bar{\theta}_{n,m}(z) := \frac{1}{m} \sum_{j=1}^m \theta_{n,j}^*(z)$, where $\theta_{n,j}^*$ is the maximum likelihood estimator in the j th subset,

and the corresponding confidence intervals as defined in (4). We only considered the situation where $m \in \{5, 10\}$ is fixed with the sample size.

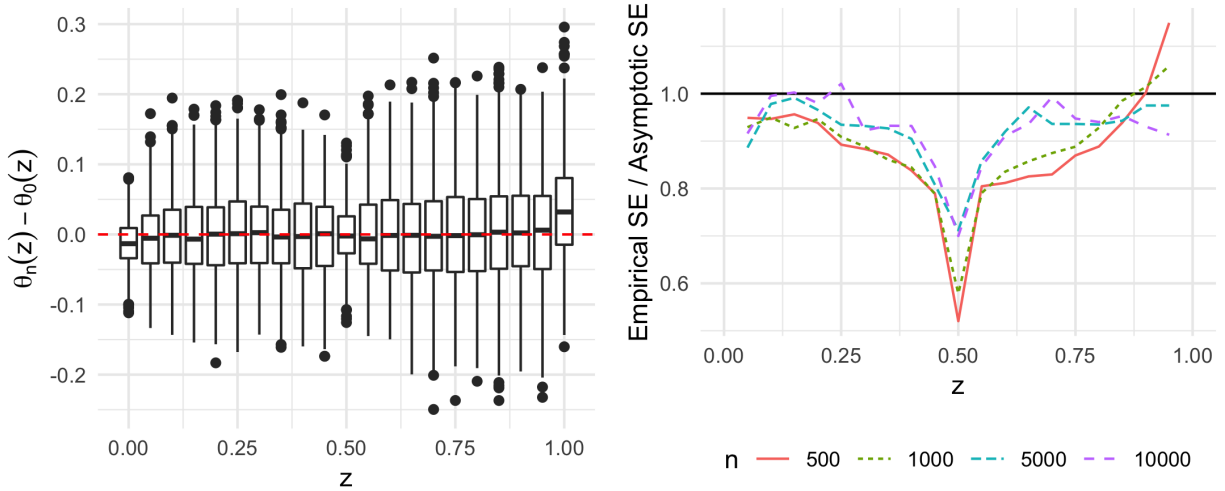


Figure 2: Left: boxplots of $\theta_n^*(z) - \theta_0(z)$ with $n = 10K$. Right: empirical standard errors of $r_n[\theta_n^*(z) - \theta_0(z)]$ divided by the limit theory-based counterparts for $z \in (0, 1)$, where $r_n = n^{1/2}$ for $z = 0.5$ and $r_n = n^{1/3}$ otherwise.

We now turn to the results of the simulation study. The left panel of Figure 2 displays the distribution of $\theta_n^*(z) - \theta_0(z)$ for $z \in [0, 1]$ and $n = 10K$. These distributions are approximately centered around 0 for $z \in (0, 1)$, but not for $z \in \{0, 1\}$. Hence, despite the positive mass at the boundaries, the maximum likelihood estimator does not appear to be consistent at the boundaries. This is a common problem among monotonicity-constrained estimators, and various correction procedures have been proposed and could be considered in this context (see, e.g. Woodroffe and Sun, 1993; Kulikov and Lopuhaä, 2006).

The right panel of Figure 2 displays the ratio of the standard deviation of $r_n[\theta_n^*(z) - \theta_0(z)]$ to the standard deviation of the asymptotic distributions derived in Section 4 for $z \neq 0, 1$. For $z = 0.5$, $r_n = n^{1/2}$ and the asymptotic distribution is that of the fully discrete case presented in Section 4.1, though we note that the results presented in that section do not apply here due to the mixed discrete-continuous nature of F_0 and G_0 here. Otherwise, $r_n = n^{1/3}$ and the asymptotic distribution is that of the continuous case presented in Section 4.2. We see that, for $z \neq 0.5$, the empirical standard error approaches the asymptotic standard deviation as n grows. However, for $z = 0.5$, the empirical standard error is converging to a limit that is strictly smaller than the asymptotic standard deviation. This suggests that, at points that have both positive mass and

positive density in a neighborhood of the point, the maximum likelihood estimator gains efficiency from the positive density. In addition, points of continuity near the mass point also experience finite-sample efficiency gains.

Figure 3 shows the ratio of the mean squared errors of the maximum smoothed likelihood estimator, the kernel density-based estimator, and the sample splitting estimators to that of the maximum likelihood estimator. The maximum smoothed likelihood estimator is slightly more efficient than the maximum likelihood estimator at continuity points, but is less efficient around mass points. Furthermore, the relative performance of the maximum likelihood estimator at positive mass points increases as the sample size grows. The kernel density estimator is generally less efficient than the maximum likelihood estimator, especially near mass points, and the discrepancy also grows with the sample size.

For large enough n , the sample splitting estimator is more efficient than the maximum likelihood estimator at all points at which the latter is consistent. The relative improvement of $\bar{\theta}_{n,m}$ grows with the number of splits m , as does the sample size n required for $\bar{\theta}_{n,m}$ to outperform θ_n^* .

Figure 4 shows the empirical coverage of 95% confidence intervals for $\theta_0(z)$ constructed using the plug-in method described in Section 4.2, the inverted likelihood ratio test approach of Banerjee and Wellner (2001), and the sample splitting approach of Banerjee et al. (2019) described above. We note that the likelihood ratio approach does not provide intervals at the end points $z = 0$ or $z = 1$. The plug-in method is conservative in large samples near mass points, but anti-conservative at some points of positive density. This is because the plug-in method is designed to work when the distributions are fully continuous, and estimation of the required nuisance parameters in the limit distribution fails in the presence of mass points. The likelihood ratio method is conservative in smaller samples, but approaches nominal coverage in large samples for points z of absolute continuity. The sample splitting method with $m = 5$ has adequate coverage for all sample sizes except for z close to the boundaries. The sample splitting method with $m = 10$ (and similarly for $m = 20$, which is not shown) appears to require very large sample sizes to attain adequate coverage over a large range of z . We note that the sample splitting methods was able to achieve good coverage in large samples at both interior absolutely continuous points and interior mass points, without the user specifying which points are which.

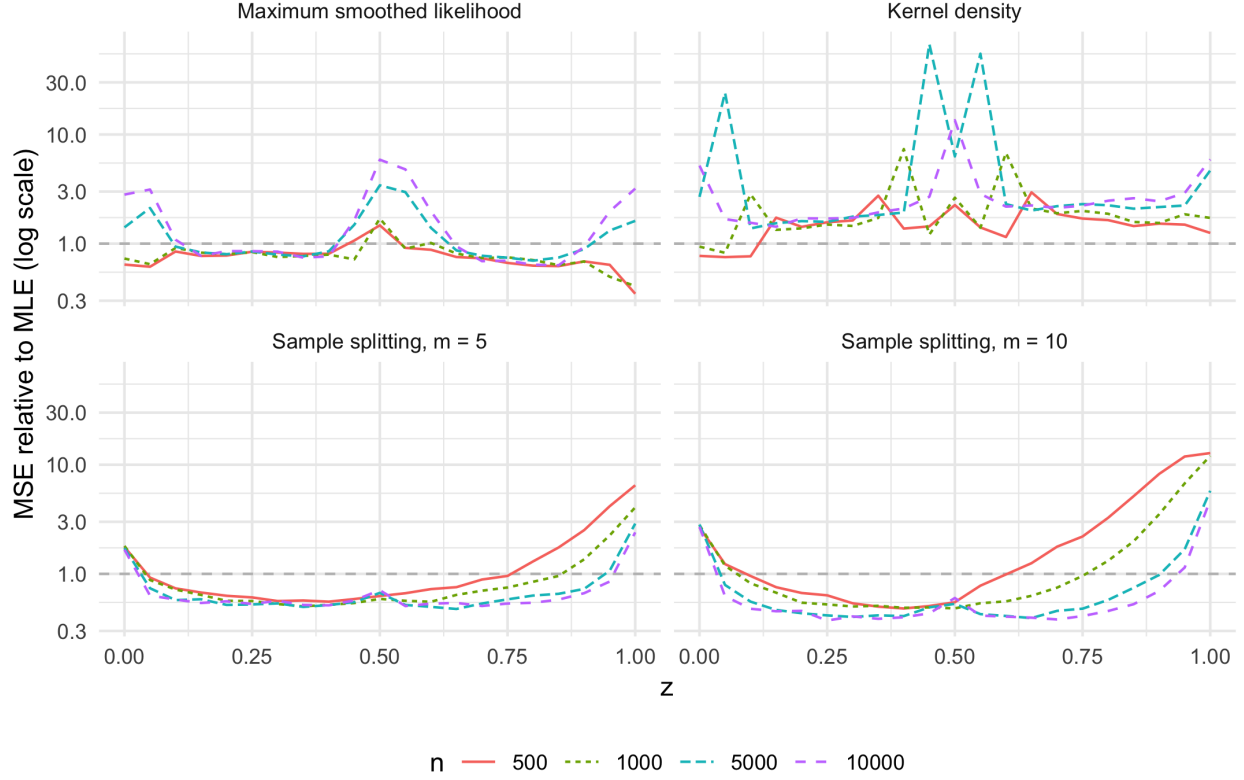


Figure 3: Relative mean squared errors of the maximum smoothed likelihood estimator, the kernel density-based estimator, and the sample splitting estimators to the maximum likelihood estimator for $z \in [0, 1]$ and various sample sizes n . The maximum likelihood has better mean squared error for y -values greater than one, and the other estimator has better mean squared error for y -values less than one.

6 Analysis of C-reactive protein for predicting bacterial infection

In this section, we use the methods presented herein to assess the use of the biomarker C-reactive protein (CRP) for determining the presence or absence of bacterial infection in children with systemic inflammatory response syndrome (SIRS). The Optimizing Antibiotic Strategies in Sepsis (OASIS) II study enrolled a prospective observational cohort of children under the age of nineteen at the pediatric intensive care unit at The Children’s Hospital of Philadelphia from August 2012 to June 2016 (Downes et al., 2018). Patients were enrolled in the study if they presented signs of SIRS, were started on a new broad-spectrum antibiotic for suspected bacterial infection, and had blood cultures taken within six hours of SIRS onset. A primary goal of the study was to assess whether CRP, which had previously been found to be predictive of bacterial infection (Downes et al., 2017),

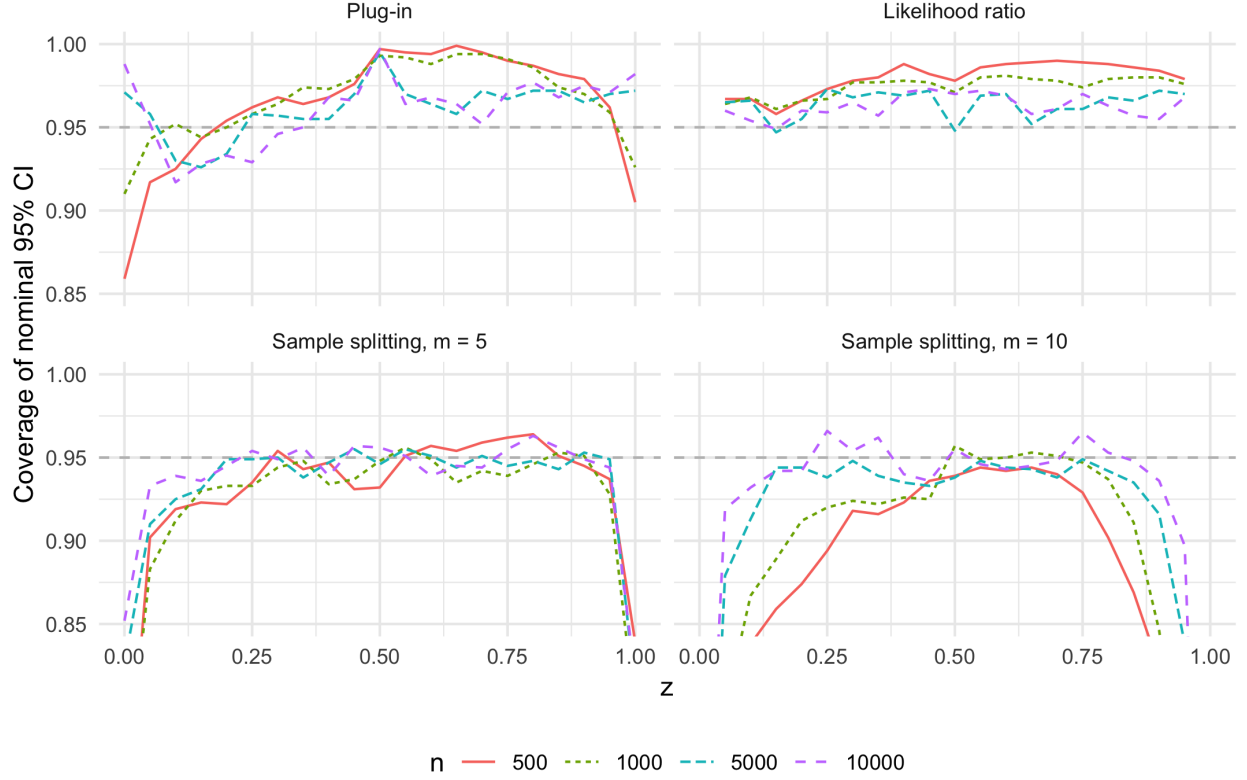


Figure 4: Coverage of 95% CIs for $z \in [0, 1]$, various sample sizes n , and four methods: the plug-in method centered around the maximum likelihood estimator (upper left), the inverted likelihood ratio tests (upper right), and the sample splitting method with $m = 5$ (lower left) and $m = 10$ (lower right). Note that the likelihood ratio method does not provide intervals at the endpoints.

could be used to determine when antibiotic therapy could be safely ended. Additional details of the study design and results of the primary analysis may be found in Downes et al. (2018).

We analyzed all patients in the OASIS II cohort with measured biomarkers and bacterial infection status to assess the odds of bacterial infection as a function of CRP value. Some patients had measurements at multiple episodes; since all such episodes were at least 30 days apart, we treated these episodes as independent of one another. We analyzed a total of $n = 504$ CRP measurements among 443 unique patients, with $n_1 = 202$ bacterial infections among 191 unique patients and $n_2 = 302$ non-infections among 266 unique patients.

Since CRP has previously been found to be predictive of bacterial infection in this patient population, there is scientific reason to believe that the density ratio order holds. We therefore computed the MLE of the density ratio function and corresponding 95% likelihood ratio-based

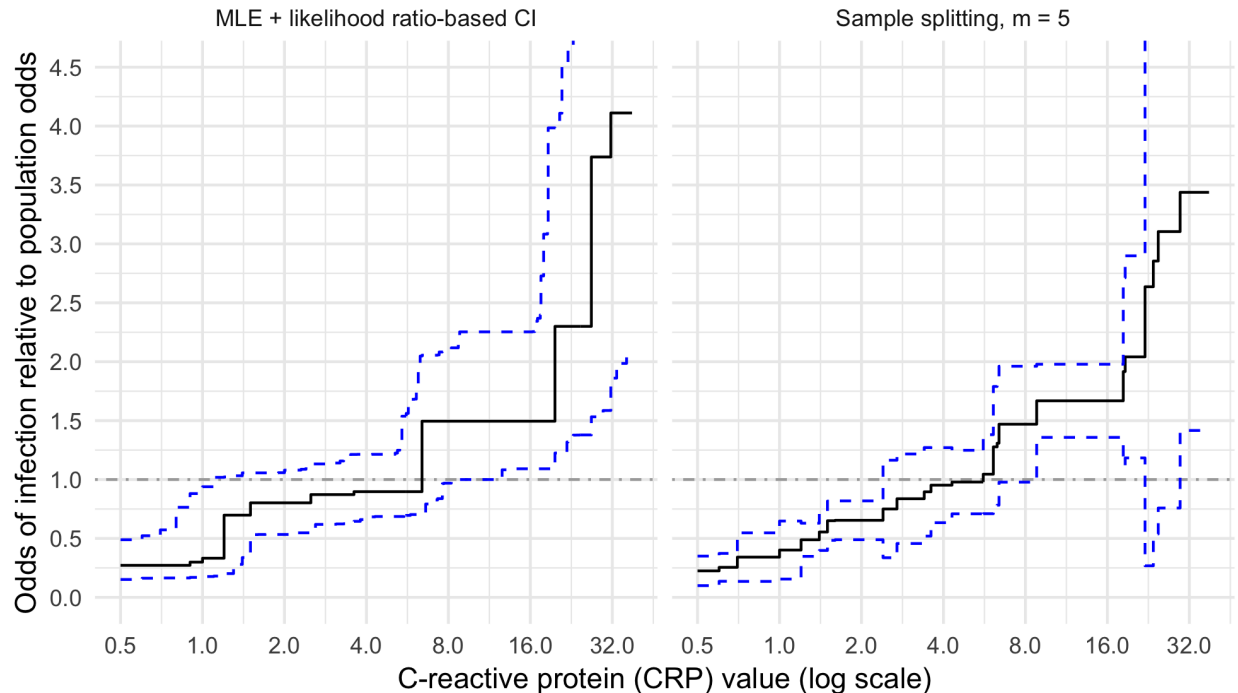


Figure 5: Odds of bacterial infection given C-reactive protein value relative to population odds in children with treating systemic inflammatory response syndrome.

pointwise confidence intervals and the sample splitting estimator of Banerjee et al. (2019) with $m = 5$ splits and corresponding 95% pointwise confidence intervals.

Figure 5 displays the estimated odds of bacterial infection given CRP value relative to the population odds of bacterial infection and 95% pointwise confidence intervals. We find that values of CRP under 1 are indicative of roughly quartered odds of infection relative to the population odds of infection, and values of CRP greater than 20 are indicative of roughly doubled odds of infection relative to the population odds. Values of CRP between 1 and 20 do not clearly indicate that a patient’s odds of infection are larger or smaller than the population odds.

Acknowledgments

The authors thank Craig Boge for help compiling the OASIS II data. The authors also gratefully acknowledge the support of the CDC Epicenters program (KJD), NICHD grant K23HD091365 (KJD), the Center for Pediatric Clinical Effectiveness and the Pediatric IDEAS Research Group of the Children’s Hospital of Philadelphia (KJD, TW), and the Department of Pediatrics of the University of Pennsylvania Perelman School of Medicine.

References

Arcones, M. A. and Samaniego, F. J. (2000). On the Asymptotic Distribution Theory of a Class of Consistent Estimators of a Distribution Satisfying a Uniform Stochastic Ordering Constraint. *Ann. Stat.*, 28(1):116–150.

- Bamber, D. (1975). The area above the ordinal dominance graph and the area below the receiver operating characteristic graph. *J. Math. Psychol.*, 12(4):387 – 415.
- Banerjee, M. (2007). Likelihood based inference for monotone response models. *Ann. Statist.*, 35(3):931–956.
- Banerjee, M., Durot, C., and Sen, B. (2019). Divide and conquer in nonstandard problems and the super-efficiency phenomenon. *Ann. Statist.*, 47(2):720–757.
- Banerjee, M. and Wellner, J. A. (2001). Likelihood ratio tests for monotone functions. *Ann. Statist.*, 29(6):1699–1731.
- Beare, B. K. and Fang, Z. (2017). Weak convergence of the least concave majorant of estimators for a concave distribution function. *Electron. J. Statist.*, 11(2):3841–3870.
- Beare, B. K. and Moon, J.-M. (2015). Nonparametric tests of density ratio ordering. *Econom. Theory*, 31(3):471–492.
- Carolan, C. A. and Tebbs, J. M. (2005). Nonparametric tests for and against likelihood ratio ordering in the two-sample problem. *Biometrika*, 92(1):159–171.
- Davidov, O. and Herman, A. (2012). Ordinal dominance curve based inference for stochastically ordered distributions. *J. R. Stat. Soc. Ser. B. Stat. Methodol.*, 74(5):825–847.
- Downes, K. J., Fitzgerald, J. C., Schriver, E., et al. (2018). Implementation of a Pragmatic Biomarker-Driven Algorithm to Guide Antibiotic Use in the Pediatric Intensive Care Unit: the Optimizing Antibiotic Strategies in Sepsis (OASIS) II Study. *J. Pediatric Infect. Dis. Soc.* advance online publication.
- Downes, K. J., Weiss, S. L., Gerber, J. S., et al. (2017). A Pragmatic Biomarker-Driven Algorithm to Guide Antibiotic Use in the Pediatric Intensive Care Unit: The Optimizing Antibiotic Strategies in Sepsis (OASIS) Study. *J. Pediatric Infect. Dis. Soc.*, 6(2):134–141.
- Dykstra, R., Kocher, S., and Robertson, T. (1995). Inference for likelihood ratio ordering in the two-sample problem. *J. Amer. Statist. Assoc.*, 90(431):1034–1040.
- Groeneboom, P. and Jongbloed, G. (2014). *Nonparametric estimation under shape constraints*. Cambridge University Press.
- Groeneboom, P. and Jongbloed, G. (2015). Nonparametric confidence intervals for monotone functions. *Ann. Statist.*, 43(5):2019–2054.
- Groeneboom, P. and Wellner, J. A. (2001). Computing Chernoff’s distribution. *J. Comput. Graph. Statist.*, 10(2):388–400.
- Hsieh, F. and Turnbull, B. W. (1996). Nonparametric and semiparametric estimation of the receiver operating characteristic curve. *Ann. Statist.*, 24(1):25–40.
- Kulikov, V. N. and Lopuhaä, H. P. (2006). The behavior of the NPMLE of a decreasing density near the boundaries of the support. *Ann. Statist.*, 34(2):742–768.
- Lehmann, E. L. and Rojo, J. (1992). Invariant Directional Orderings. *Ann. Statist.*, 20(4):2100–2110.
- Mukerjee, H. (1996). Estimation of survival functions under uniform stochastic ordering. *J. Amer. Statist. Assoc.*, 91(436):1684–1689.
- Rojo, J. and Samaniego, F. J. (1991). On nonparametric maximum likelihood estimation of a distribution uniformly stochastically smaller than a standard. *Statist. Probab. Lett.*, 11(3):267 – 271.
- Rojo, J. and Samaniego, F. J. (1993). On estimating a survival curve subject to a uniform stochastic ordering constraint. *J. Amer. Statist. Assoc.*, 88(422):566–572.
- Roosen, J. and Hennessy, D. A. (2004). Testing for the monotone likelihood ratio assumption. *J. Bus. Econ. Stat.*, 22(3):358–366.
- Shaked, M. and Shanthikumar, J. G. (2007). *Stochastic Orders*. Springer Science & Business Media.

- Tang, C.-F., Wang, D., and Tebbs, J. M. (2017). Nonparametric goodness-of-fit tests for uniform stochastic ordering. *Ann. Statist.*, 45(6):2565–2589.
- Westling, T. and Carone, M. (2019). A unified study of nonparametric inference for monotone functions. *Ann. Statist.* Advance online publication.
- Woodroffe, M. and Sun, J. (1993). A penalized maximum likelihood estimate of $f(0+)$ when f is non-increasing. *Statist. Sinica*, 3(2):501–515.
- Yu, T., Li, P., and Qin, J. (2017). Density estimation in the two-sample problem with likelihood ratio ordering. *Biometrika*, 104(1):141–152.

Supplementary Material

Proof of Theorems

Proof of Theorem 1. We first suppose that $F \ll G$ and ν is non-decreasing on \mathcal{G} , and we show that $R_{F,G}$ is convex on $\text{Im}(G)$. Since $F \ll G$, we have that $F(x) = \int_{-\infty}^x \nu(u) dG(u)$ for all x . Let $t, u, v \in \text{Im}(G)$, where $t < v$ and $u = \lambda t + (1 - \lambda)v$ for $\lambda \in (0, 1)$. We then have by the monotonicity of ν that

$$\begin{aligned} [R_{F,G}(v) - R_{F,G}(u)] &= \int_{G^-(u)}^{G^-(v)} \nu(z) dG(z) \\ &\geq \nu(G^-(u)) [G(G^-(v)) - G(G^-(u))] \\ &\geq \int_{G^-(t)}^{G^-(u)} \nu(z) dG(z) \frac{G(G^-(v)) - G(G^-(u))}{G(G^-(u)) - G(G^-(t))} \\ &= [R_{F,G}(u) - R_{F,G}(t)] \frac{G(G^-(v)) - G(G^-(u))}{G(G^-(u)) - G(G^-(t))}. \end{aligned}$$

Noting that $G(G^-(z)) = z$ for any $z \in \text{Im}(G)$ and that $v - u = \lambda(v - t)$ and $u - t = (1 - \lambda)(v - t)$, we then have $(1 - \lambda) [R_{F,G}(v) - R_{F,G}(u)] \geq \lambda [R_{F,G}(u) - R_{F,G}(t)]$, which implies that $\lambda R_{F,G}(t) + (1 - \lambda) R_{F,G}(v) \geq R_{F,G}(u)$, which proves the claim.

Next, we suppose that $F \ll G$, $R := R_{F,G}$ is convex on $\text{Im}(G)$, and ν is continuous on \mathcal{G} , and we show that ν is nondecreasing on \mathcal{G} . The basic argument amounts to using convexity of R to compare the slopes of chords or sequences of chords, and to relate these slopes to values of ν . Let $x, y \in \mathcal{G}$ with $x < y$. Suppose that we can find sequences $\{z_j\}_{j \geq 1}$ and $\{w_j\}_{j \geq 1}$ such that $s_j := [R(G(x)) - R(G(z_j))]/[G(x) - G(z_j)]$ converges to $\nu(x)$, $t_j := [R(G(y)) - R(G(w_j))]/[G(y) - G(w_j)]$ converges to $\nu(y)$, and $z_j \leq w_j$ for all j large enough. Then, by convexity of R , $s_j \leq t_j$ for all j large enough, which implies that $\nu(x) \leq \nu(y)$. The exact form of $\{z_j\}_{j \geq 1}$ and $\{w_j\}_{j \geq 1}$ depends on how G looks near x and y . In particular, there are three cases for y : (1) $G(y) > G(y-)$ and there exists $p \in [x, y)$ such that $G(y-) = G(p)$; (2) $G(y) > G(y-)$ but there is no $p \in [x, y)$ such that $G(y-) = G(p)$; and (3) $G(y) = G(y-)$. We begin by specifying $\{w_j\}_{j \geq 1}$ in each case.

In case (1), we take $w_j = p$ for all j . Since $F \ll G$, we must have $F(G^-(G(p))) = F(y-)$, so that $t_j = \nu(y)$ for all j . In case (2), it must be that $G^-(G(y-)) = y$. In this case, there exists $\{w_j\}_{j \geq 1}$ increasing to y such that $w_j \in (x, y) \cap \mathcal{G}$ for each j , $G(w_j)$ increases to $G(y-)$ and $F(w_j)$ increases to $F(y-)$. We then have that $R(G(w_j))$ increases to $F(G^-(G(y-))) = F(y-)$, so that t_j increases to $[F(y) - F(y-)]/[G(y) - G(y-)] = \nu(y)$. In case (3), we first note that $F(G^-(G(y))) = F(y)$ since $F \ll G$. Additionally, since $y \in \mathcal{G}$, there exist $\{w_j\}_{j \geq 1}$ in \mathcal{G} with $G^-(G(w_j)) = w_j$ for each j that either (a) increases to y and $G(w_j) < G(y)$ for each j , or (b) decreases to y and $G(w_j) > G(y)$ for each j . In either case, we have

$$t_j = \frac{\int_{w_j}^y \nu(u) dG(u)}{G(y) - G(w_j)} = \nu(y) + \frac{\int_{w_j}^y [\nu(u) - \nu(y)] dG(u)}{G(y) - G(w_j)}.$$

For any $\varepsilon > 0$, by continuity of ν over \mathcal{G} , we can find m such that $j \geq m$ implies $|\nu(u) - \nu(y)| < \varepsilon$ for all $u \in [w_j, y] \cap \mathcal{G}$. If (a) holds and t_j is bounded above, we then have $\int_{w_j}^y |\nu(u) - \nu(y)| dG(u) \leq \varepsilon [G(y) - G(w_j)]$ for all $j \geq m$, so that then $\lim_{j \rightarrow \infty} t_j = \nu(y)$. If t_j is not bounded above then $\nu(y) = +\infty$, so that $\nu(x) \leq \nu(y)$ trivially. If (b) holds then t_j is bounded below by zero, so by a similar calculation $\lim_{j \rightarrow \infty} t_j = \nu(y)$.

The three cases for x are similar: (1) $G(x) > G(x-)$ and there exists $q \in [-\infty, x)$ such that

$G(x-) = G(q)$; (2) $G(x) > G(x-)$ but there is no such q ; and (3) $G(x) = G(x-)$. In case (1), we take $z_j = q$ for all j . Since $F \ll G$, we must have $F(G^-(G(q))) = F(x-)$, so that $s_j = \nu(y)$ for all j . In case (2), it must be that $G^-(G(x-)) = x$, and again there exists an increasing sequence $\{z_j\}_{j \geq 1}$ increasing to x such that $z_j \in (-\infty, x) \cap \mathcal{G}$ for each j , $G(z_j)$ increases to $G(x-)$ and $F(z_j)$ increases to $F(x-)$. We then have that $R(G(z_j))$ increases to $F(x-)$, so that s_j increases to $\nu(x)$. In case (3), $F(G^-(G(x))) = F(x)$, and since $x \in \mathcal{G}$, there exists $\{z_j\}_{j \geq 1}$ in \mathcal{G} with $G^-(G(z_j)) = z_j$ for each j that either (a) increases to x and $G(z_j) < G(x)$ for each j , or (b) decreases to x and $G(z_j) > G(x)$ for each j . If (a) holds and s_j is bounded above, then s_j converges to $\nu(x)$ by continuity of ν as before. If s_j is not bounded above then s_j converges to $\nu(x) = +\infty$. If (b) holds then s_j is bounded below by zero, so again $\lim_{j \rightarrow \infty} s_j = \nu(x)$.

Of the nine pairings of cases for y and cases for x , the only situation in which it is not immediately clear that $z_j \leq w_j$ for all j large enough is that z_j decreases to x (case 3b) and $w_j = p$ for all j (case 1). However, we note that $x = p$ if and only if $G(x) = G(y-)$, which would imply that case (3b) cannot hold for x . Therefore, if z_j decreases to x and $w_j = p$, then $p > x$, so that $z_j < w_j$ for all j large enough. This completes the argument.

Finally, we address statement (2) of the result: we suppose that $F \ll G$ and ν is continuous and non-decreasing on \mathcal{G} , and we show that $\theta_{F,G} = \nu$ on \mathcal{G} . By (1), R is convex on $\text{Im}(G)$. First, we claim that $\text{GCM}_{[0,1]}(R) = H$, where $H : [0, 1] \rightarrow [0, 1]$ takes the following form. For any $u \in \text{Im}(G)$, $H(u) := R(u)$. If $u \notin \text{Im}(G)$, then there exists $x \in \mathbb{R}$ and $\lambda \in [0, 1]$ such that $u = \lambda G(x-) + (1 - \lambda)G(x)$. We then define $H(u) := \lambda R(G(x-)) + (1 - \lambda)R(G(x))$. Thus, H is the linear interpolation of $R|_{\text{Im}(G)}$ to $[0, 1]$. In order to show that H indeed equals $\text{GCM}_{[0,1]}(R)$, we need to show that (a) H is convex, (b) $H \leq R$, and (c) $H \geq \bar{H}$ for any other convex minorant of R .

For (a), we let $u, v \in [0, 1]$ and $p = \lambda u + (1 - \lambda)v$ for $\lambda \in (0, 1)$. There then exist $u_1 \leq u_2 \leq p_1 \leq p_2 \leq v_1 \leq v_2$ which are all elements of $\text{Im}(G)$ and $\lambda_1, \lambda_2, \lambda_3 \in [0, 1]$ such that $u = \lambda_1 u_1 + (1 - \lambda_1)u_2$, $v = \lambda_2 v_1 + (1 - \lambda_2)v_2$, and $p = \lambda_3 p_1 + (1 - \lambda_3)p_2$, and furthermore $H(u) = \lambda_1 R(u_1-) + (1 - \lambda_1)R(u_2)$, $H(v) = \lambda_2 R(v_1-) + (1 - \lambda_2)R(v_2)$, and $H(p) = \lambda_3 R(p_1-) + (1 - \lambda_3)R(p_2)$. The remainder of the argument is best seen with a picture. Let U be the point $(u, H(u))$, U_1 be the point $(u_1, H(u_1))$, and so on. By convexity of R , the line segment $\overline{P_1 P_2}$ lies below or on the line segment $\overline{U_2 V_1}$, which lies below or on $\overline{UV_1}$, which lies below or on \overline{UV} . Therefore, $(p, H(p))$, which falls on $\overline{P_1 P_2}$, is no greater than $(p, \lambda H(u) + (1 - \lambda)H(v))$, which falls on \overline{UV} .

For (b), by definition, $H(u) = R(u)$ for any $u \in \text{Im}(G)$. If $u \notin \text{Im}(G)$, then $u = \lambda G(x-) + (1 - \lambda)G(x)$, and hence $G^-(u) = G^-(G(x)) = x$. As a result, $R(u) = R(G(x)) > H(u) = \lambda R(G(x-)) + (1 - \lambda)R(G(x))$.

We have now shown that H is a convex minorant of R . For (c), if \bar{H} is another convex minorant of R , then clearly $H(u) \geq \bar{H}(u)$ for all $u \in \text{Im}(G)$. If $u \notin \text{Im}(G)$, then $u = \lambda G(x-) + (1 - \lambda)G(x)$. If $G(x-) \in \text{Im}(G)$, then $\bar{H}(u) \leq \lambda \bar{H}(G(x-)) + (1 - \lambda)\bar{H}(G(x)) \leq \lambda R(G(x-)) + (1 - \lambda)R(G(x)) = H(u)$. If $G(x-) \notin \text{Im}(G)$, then there must be an $\varepsilon > 0$ such that $z \in \text{Im}(G)$ for all $z \in (G(x-) - \varepsilon, G(x-))$, so that $\bar{H}(u) \leq \lambda(z)R(z-) + (1 - \lambda(z))R(G(x))$ for each $z \in (G(x-) - \varepsilon, G(x-))$, where $\lambda(z) \in (0, 1)$ and $\lambda(z) \rightarrow \lambda$ as $z \rightarrow G(x-)$. Taking the limit as $z \rightarrow G(x-)$, we have that $\bar{H}(u) \leq \lambda R(G(x-)) + (1 - \lambda)R(G(x)) = H(u)$.

We now have that $\theta_{F,G}(x) = (\partial_- H)(G(x))$, so it remains to show that $(\partial_- H)(G(x)) = \nu(x)$ for all $x \in \mathcal{G}$. First, if $G(x) > G(x-)$, then $H(u) = \lambda R(G(x-)) + (1 - \lambda)R(G(x)) = \lambda F(x-) + (1 - \lambda)F(x)$ for all $u = \lambda G(x-) + (1 - \lambda)G(x)$ for $\lambda \in (0, 1)$. Therefore, $(\partial_- H)(u) = [F(x) - F(x-)]/[G(x) - G(x-)] = \nu(x)$ for all such u , so that $(\partial_- H)(G(x)) = \nu(x)$. If instead $x \in \mathcal{G}$ and $G(x) = G(x-)$ then $H(G(x)) = R(G(x))$, and it is straightforward to see from the definition of R that $(\partial_- R)(G(x)) = \nu(x)$. \square

Proof of Theorem 2. We first note that $L_n(F, G) = 0$ for any G such that $G(Y_j) = G(Y_j-)$ for any $j \in \{1, \dots, n_2\}$. As a result, we may restrict our attention to G such that $G(Y_j) > G(Y_j-)$ for all j , which implies that G^- has support at each $G(Y_j)$. For any such G , we define $\bar{G} := G \circ L$, where $L(y) := \max\{Y_j : Y_j \leq y\}$. We then have $\bar{G}(Y_j) - \bar{G}(Y_j-) \geq G(Y_j) - G(Y_j-)$ for each j . Furthermore, the support of \bar{G}^- is $\{G(Y_j) : j = 1, \dots, n_2\}$ is contained in the support of G , $\bar{G}(Y_j) = G(Y_j)$ for each j , and $F \circ G^-$ is by assumption convex on the support of G^- . Therefore, $F \circ \bar{G}^-$ is convex on the support of \bar{G}^- , so that $(F, \bar{G}) \in \mathcal{M}_0$ and $L_n(F, \bar{G}) \geq L_n(F, G)$. Hence, we may further restrict our attention to G which are discrete with jumps at Y_1, \dots, Y_{n_2} . By a similar argument, we can restrict our attention to F which are discrete with jumps at X_1, \dots, X_{n_1} or Y_1, \dots, Y_{n_2} .

We define $y_0 := -\infty$, and $u_j := G(y_j)$, so that the support of G^- for any discrete G with jumps at Y_1, \dots, Y_{n_2} is $\{u_j : j = 0, \dots, m_2\}$, and $G^-(u_j) = y_j$. Defining $g_j := u_j - u_{j-1}$ and s_j the number of Y_k such that $Y_k = y_j$, we have $\prod_{j=1}^{n_2} [G(Y_j) - G(Y_j-)] = \prod_{j=1}^{m_2} g_j^{s_j}$. We then define $f_j := F(y_j) - F(y_j-)$ for each j , and we note that $(F, G) \in \mathcal{M}_0$ if and only if $f_1/g_1 \leq f_2/g_2 \leq \dots \leq f_{m_2}/g_{m_2}$. Suppose that the values f_1, \dots, f_{m_2} are fixed in such a way as to satisfy these constraints. We denote by $\mathcal{J}_j := \{k : x_k \in (y_{j-1}, y_j]\}$ for $j = 1, \dots, m_2 + 1$, where $y_{m_2+1} := +\infty$, and by r_i the number of X_k such that $X_k = x_i$. Noting that $\mathcal{J}_1, \dots, \mathcal{J}_{m_2+1}$ are disjoint with union $\{1, \dots, m_1\}$, we then have

$$\prod_{i=1}^{n_1} [F(X_i) - F(X_i-)] = \prod_{j=1}^{m_2+1} \prod_{k \in \mathcal{J}_j} [F(x_k) - F(x_k-)]^{r_k}.$$

Additionally, for each $j \in \{1, \dots, m_2 + 1\}$, we must have that $\sum_{k \in \mathcal{J}_j} [F(x_k) - F(x_k-)] = f_j$. Therefore, maximizing $L_n(F, G)$ with respect to F with f_1, \dots, f_{m_2+1} fixed amounts to maximizing $\prod_{k \in \mathcal{J}_j} [F(x_k) - F(x_k-)]^{r_k}$ subject to $\sum_{k \in \mathcal{J}_j} [F(x_k) - F(x_k-)] = f_j$ for each j . This implies that a maximizer F_n^* must satisfy

$$F_n^*(x_k) - F_n^*(x_k-) = f_j \frac{r_k}{\sum_{l \in \mathcal{J}_j} r_l}$$

for each $x_k \in \mathcal{J}_j$. Therefore, $\prod_{k \in \mathcal{J}_j} [F_n^*(x_k) - F_n^*(x_k-)]^{r_k}$ is proportional to $\prod_{k \in \mathcal{J}_j} f_j^{r_k} = f_j^{R_j}$ for $R_j := \sum_{k \in \mathcal{J}_j} r_k$, which is the number of X_i in the interval $(y_{j-1}, y_j]$.

We note that if there are j such that no $x_k \in (y_j, y_{j+1}]$ but $f_j > 0$, then there are infinitely many maximizers because any F_n^* that assigns mass f_j to the interval $(y_{j-1}, y_j]$ yields the same likelihood and satisfies the constraints. In these cases, for the sake of uniqueness we will put mass f_j at the point y_j .

We have at this point reduced the problem to maximizing

$$\left\{ \prod_{k=1}^{m_2+1} f_k^{R_k} \right\} \left\{ \prod_{k=1}^{m_2} g_k^{s_k} \right\} = \left\{ \prod_{k=1}^{m_2} f_k^{R_k} g_k^{s_k} \right\} f_{m_2+1}^{R_{m_2+1}}$$

subject to $f_1/g_1 \leq f_2/g_2 \leq \dots \leq f_{m_2}/g_{m_2}$ and $\sum_{k=1}^{m_2} g_k = \sum_{k=1}^{m_2+1} f_k = 1$. Letting $\bar{f}_k := f_k/(1 - f_{m_2+1})$ for $k \leq m_2$, this is equivalent to maximizing

$$\bar{L}_n(\bar{f}_1, \dots, \bar{f}_{m_2}, f_{m_2+1}, g_1, \dots, g_{m_2}) := \left\{ \prod_{k=1}^{m_2} \bar{f}_k^{R_k} g_k^{s_k} \right\} (1 - f_{m_2+1})^{n_1 - R_{m_2+1}} f_{m_2+1}^{R_{m_2+1}}$$

subject to $\bar{f}_1/g_1 \leq \bar{f}_2/g_2 \leq \dots \leq \bar{f}_{m_2}/g_{m_2}$ and $\sum_{k=1}^{m_2} g_k = \sum_{k=1}^{m_2} \bar{f}_k = 1$. The term involving f_{m_2+1} is maximized for $f_{m_2+1}^* = R_{m_2+1}/n_1 = 1 - F_n(y_{m_2})$.

From this point we take a similar approach to that in Dykstra et al. (1995). We define $\bar{n}_1 := \sum_{k=1}^{m_2} R_k = F_n(y_{m_2})n_1$, $\sigma_k := \bar{n}_1 \bar{f}_k + n_2 g_k$ and $\rho_k := \bar{n}_1 \bar{f}_k / \sigma_k$, so that $\bar{f}_k = \rho_k \sigma_k / \bar{n}_1$ and $g_k = (1 - \rho_k) \sigma_k / n_2$. Optimizing \bar{L}_n with respect to $\bar{f}_1, \dots, \bar{f}_{m_2}$ and g_1, \dots, g_{m_2} such that $\sum_{k=1}^{m_2} \bar{f}_k = \sum_{k=1}^{m_2} g_k = 1$ and $\bar{f}_1/g_1 \leq \bar{f}_2/g_2 \leq \dots \leq \bar{f}_{m_2}/g_{m_2}$ is equivalent to optimizing

$$\bar{L}_n(\boldsymbol{\rho}, \boldsymbol{\sigma}) = \prod_{k=1}^{m_2} [\rho_k \sigma_k / \bar{n}_1]^{R_k} [(1 - \rho_k) \sigma_k / n_2]^{s_k} = \bar{n}_1^{-\bar{n}_1} n_2^{-n_2} \prod_{k=1}^{m_2} \rho_k^{R_k} (1 - \rho_k)^{s_k} \prod_{k=1}^{m_2} \sigma_k^{R_k + s_k}$$

such that $\sum_{k=1}^{m_2} \rho_k \sigma_k = \bar{n}_1$, $\sum_{k=1}^{m_2} \sigma_k = \bar{n}_1 + n_2$, and $\rho_1 \leq \dots \leq \rho_{m_2}$, where $\boldsymbol{\rho} := (\rho_1, \dots, \rho_{m_2})$ and $\boldsymbol{\sigma} := (\sigma_1, \dots, \sigma_{m_2})$.

Now, $\prod_{k=1}^{m_2} \sigma_k^{R_k + s_k}$ such that $\sum_{k=1}^{m_2} \sigma_k = \bar{n}_1 + n_2$ is maximized for $\sigma_k^* = R_k + s_k$. Next, maximizing $\prod_{k=1}^{m_2} \rho_k^{R_k} (1 - \rho_k)^{s_k}$ with respect to $\rho_1 \leq \dots \leq \rho_{m_2}$ is equivalent to maximizing

$$\sum_{k=1}^{m_2} [R_k \log \rho_k + s_k \log(1 - \rho_k)] = \sum_{k=1}^{m_2} w_k [t_k \log \rho_k + (1 - t_k) \log(1 - \rho_k)]$$

for $w_k := R_k + s_k \geq 1$ and $t_k := R_k / w_k$. By Theorem 2.1 and Exercise 2.21 of Groeneboom and Jongbloed (2014), the maximizer $(\rho_1^*, \dots, \rho_{m_2}^*)$ of this expression over all $\rho_1 \leq \dots \leq \rho_{m_2}$ is given by the weighted isotonic regression of t_1, \dots, t_{m_2} with weights w_1, \dots, w_{m_2} . By Lemma 2.1 of Groeneboom and Jongbloed (2014), ρ_k^* is equal to the left derivative of the GCM of the set of points

$$\{(0, 0)\} \cup \left\{ \left(\sum_{j=1}^k w_j, \sum_{j=1}^k t_j w_j \right) : k = 1, \dots, m_2 \right\} = \{(n_1 F_n(y_k) + n_2 G_n(y_k), n_1 F_n(y_k)) : k = 0, \dots, m_2\}$$

evaluated at $n_1 F_n(y_k) + n_2 G_n(y_k)$. We note that $\sum_{k=1}^{m_2} w_k \rho_k^* = \sum_{k=1}^{m_2} \sigma_k^* \rho_k^* = n_1 F(y_{m_2}) = \bar{n}_1$. Therefore, we have that $L_n(\boldsymbol{\rho}, \boldsymbol{\sigma}) \leq L_n(\boldsymbol{\rho}^*, \boldsymbol{\sigma}^*)$ for all $\boldsymbol{\rho}$ such that $\rho_1 \leq \dots \leq \rho_{m_2}$ and $\boldsymbol{\sigma}$ such that $\sum_{k=1}^{m_2} \sigma_k = \bar{n}_1 + n_2$. Since $\boldsymbol{\rho}^*$ and $\boldsymbol{\sigma}^*$ also satisfy $\sum_{k=1}^{m_2} \sigma_k^* \rho_k^* = \bar{n}_1$, this implies that $(\boldsymbol{\rho}^*, \boldsymbol{\sigma}^*)$ is an optimizer of \bar{L}_n over the set of stated constraints.

We now have that $f_k^* = (R_k + s_k)(\rho_k^* / n_1)$ and $g_k^* = (R_k + s_k)(1 - \rho_k^*) / n_2$. Since $w_k = R_k + s_k$, this implies that $F_n^*(y_k) = \bar{A}_k / n_1$ and $G_n^*(y_k) = [n_2 G_n(y_k) + n_1 F_n(y_k) - \bar{A}_k] / n_2$, where \bar{A}_k is the value of the GCM of the set of points defined above at $n_1 F_n(y_k) + n_2 G_n(y_k)$. We note that $\bar{A}_k / n_1 = A_k^*$, for A_k^* the value of the GCM of $\{(\pi_n F_n(y_k) + (1 - \pi_n) G_n(y_k), F_n(y_k)) : k = 0, \dots, m_2\}$ evaluated at $\pi_n F_n(y_k) + (1 - \pi_n) G_n(y_k)$. Additionally, $[n_2 G_n(y_k) + n_1 F_n(y_k) - \bar{A}_k] / n_2 = B_k^*$ for B_k^* the value of the LCM of $\{(\pi_n F_n(y_k) + (1 - \pi_n) G_n(y_k), G_n(y_k)) : k = 0, \dots, m_2\}$ at $\pi_n F_n(y_k) + (1 - \pi_n) G_n(y_k)$. \square

Proof of Corollary 1. From the proof of Theorem 2, we have that $F_n^*(y_k) = A_k^*$ and $G_n^*(y_k) = G_n(y_k) + \frac{\pi_n}{1 - \pi_n} [F_n(y_k) - A_k^*]$. Let j'_0, \dots, j'_K denote the indices of the vertices of the GCM of $\{(\pi_n F_n(y_k) + (1 - \pi_n) G_n(y_k), F_n(y_k)) : k = 0, \dots, m_2\}$. Then $F_n^*(y_{j'_k}) = F_n(y_{j'_k})$ for each $k = 0, \dots, K$ and $G_n^*(y_{j'_k}) = G_n(y_{j'_k})$. It is also straightforward to see that $\{(h_k, A_k) : k = 0, \dots, m_2\}$ is a convex minorant of $\{(h_k, F_n(y_k)) : k = 0, \dots, m_2\}$ if and only if $\{(G_n(y_k), A_k) : k = 0, \dots, m_2\}$ is a convex minorant of $\{(G_n(y_k), F_n(y_k)) : k = 0, \dots, m_2\}$. Therefore, $\{(F_n(y_{j'_k}), G_n(y_{j'_k})) : k = 0, \dots, K\}$ form the vertices of the GCM of $\{(G_n(y_k), F_n(y_k)) : k = 0, \dots, m_2\}$. \square

Proof of Theorem 3. The conditions of Theorem 1 of Westling and Carone (2019) are satisfied by the uniform consistency of empirical distribution functions. \square

Proof of Theorem 4. This result follows by the delta method, as discussed in the text. \square

Additional simulations: discrete case

We now present results from a numerical study of the properties of the maximum likelihood estimator in the case where both F_0 and G_0 are fully discrete. We set F_0 and G_0 as the distribution functions of Poisson random variables with rates 6 and 4, respectively, and we set π_0 to 0.4. We simulated 1000 datasets each for $n \in \{500, 1000, 5000, 10000\}$ and estimated the maximum likelihood estimator θ_n^* , the empirical mass ratio function, defined as the ratio of the empirical mass functions of X_1, \dots, X_{n_1} and Y_1, \dots, Y_{n_2} , and the sample splitting estimators with $m \in \{5, 10, 20\}$ (Banerjee et al., 2019). We computed Wald-type confidence intervals (constructed around $\log \theta_n^*$ and exponentiated) using the asymptotic variance provided in Section 4.1 of the main text, likelihood ratio-based confidence intervals, and confidence intervals around the sample splitting estimators as outlined in Section 5 of the main text.

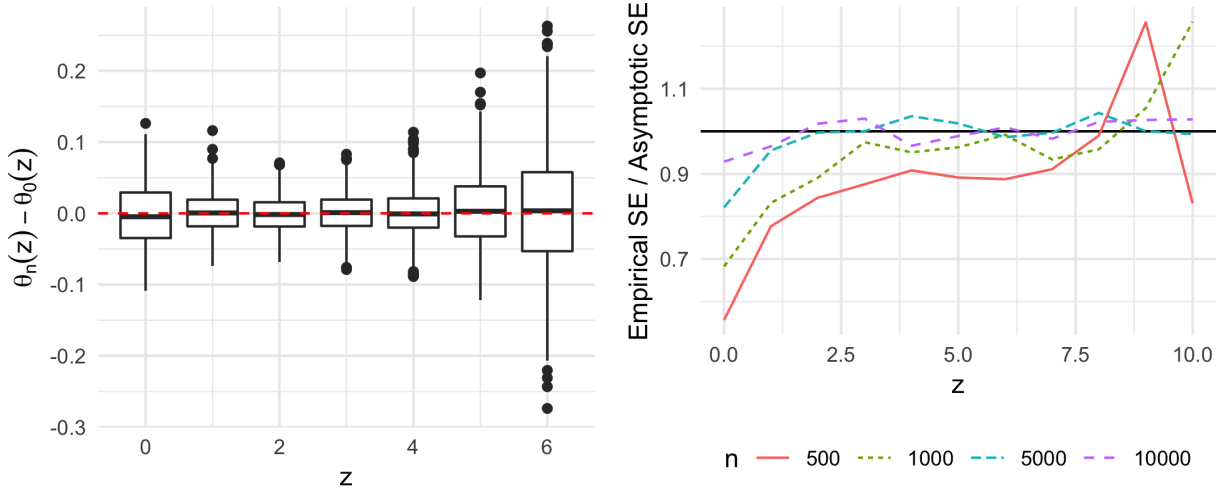


Figure 6: Left: boxplots of $\theta_n^*(z) - \theta_0(z)$ with $n = 10K$ in the fully discrete case. Right: empirical standard errors of $n^{1/2}[\theta_n^*(z) - \theta_0(z)]$ divided by the limit theory-based counterparts for $z \in \{0, 1, \dots, 10\}$.

The left panel of Figure 6 displays the distribution of $\theta_n^*(z) - \theta_0(z)$ for $z \in \{0, 1, \dots, 6\}$, and demonstrates that θ_n^* is approximately unbiased in large samples. The right panel of Figure 6 displays the ratio of the empirical standard deviation of $n^{1/2}[\theta_n^*(z) - \theta_0(z)]$ to the standard deviation based on the asymptotic theory, and demonstrates that the empirical standard deviation of $\theta_n^*(z)$ approaches the standard deviation defined by the limit theory as the sample size grows, and that $\theta_n^*(z)$ is more efficient than the limit theory suggests in smaller samples for small values of z .

Figure 7 displays the ratio of the mean squared errors of the empirical and sample splitting estimators to that of the maximum likelihood estimator. For the empirical estimator, this ratio approaches one as sample size grows, which agrees with our theoretical result suggesting that the two estimators are asymptotically equivalent. However, in small samples, the maximum likelihood estimator has strictly smaller mean squared error than the empirical estimator. The mean squared errors of the sample splitting estimators also approach that of the maximum likelihood estimator as the sample size grows, which is concurrent with existing theory for $n^{-1/2}$ -rate asymptotics.

Figure 8 shows the empirical coverage of 95% confidence intervals for $\theta_0(z)$ constructed using Wald-type confidence intervals with a plug-in standard error according to the results presented in Section 4.1 of the main text, the inverted likelihood ratio test approach of Banerjee and Wellner (2001), and the sample splitting approach of Banerjee et al. (2019) described in the main text. We

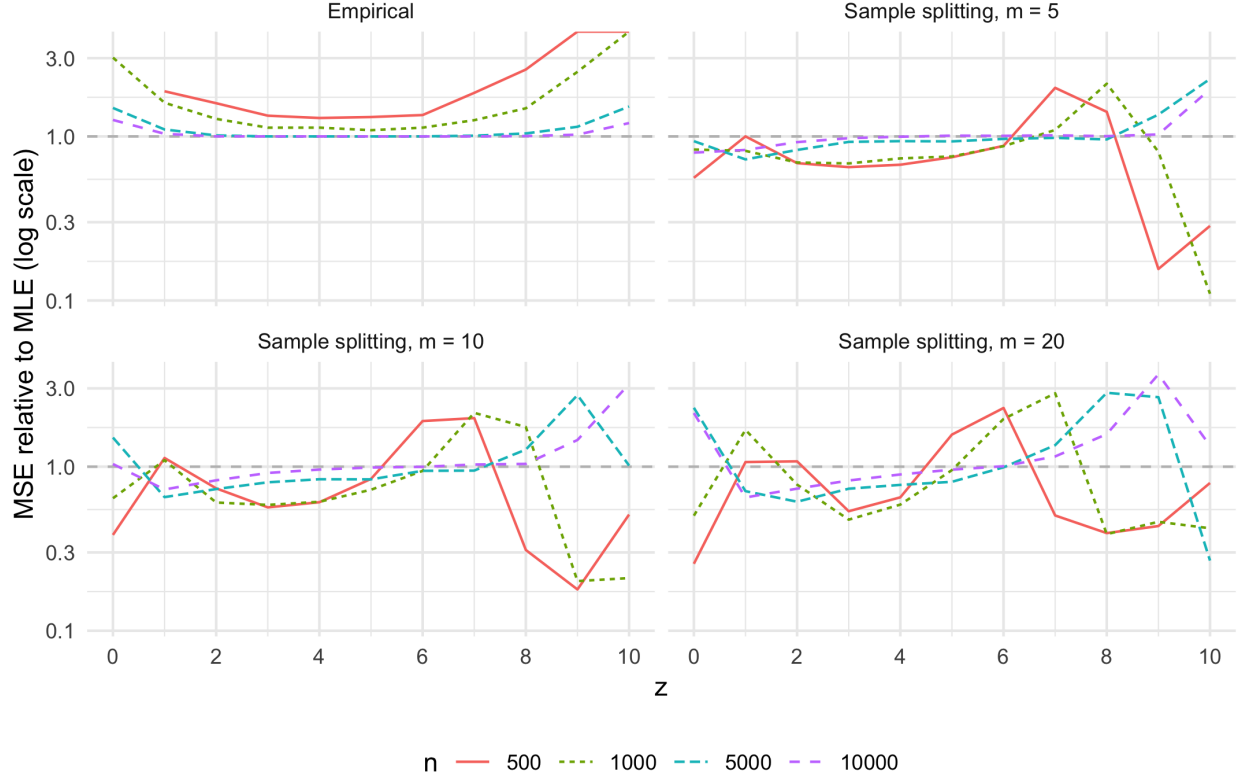


Figure 7: Relative mean squared errors of the empirical estimator and the sample splitting estimators to the maximum likelihood estimator for $z \in \{0, 1, \dots, 10\}$ and various sample sizes n in the fully discrete case. The maximum likelihood has better mean squared error for y -values greater than one, and the other estimator has better mean squared error for y -values less than one.

note that the likelihood ratio approach does not provide intervals at the end point $z = 0$. The plug-in method is conservative in small samples, but its coverage approaches 95% for $z \neq 0$ as n grows. The likelihood ratio method provides excellent coverage at all sample sizes. The sample splitting method has good coverage in large enough sample sizes.

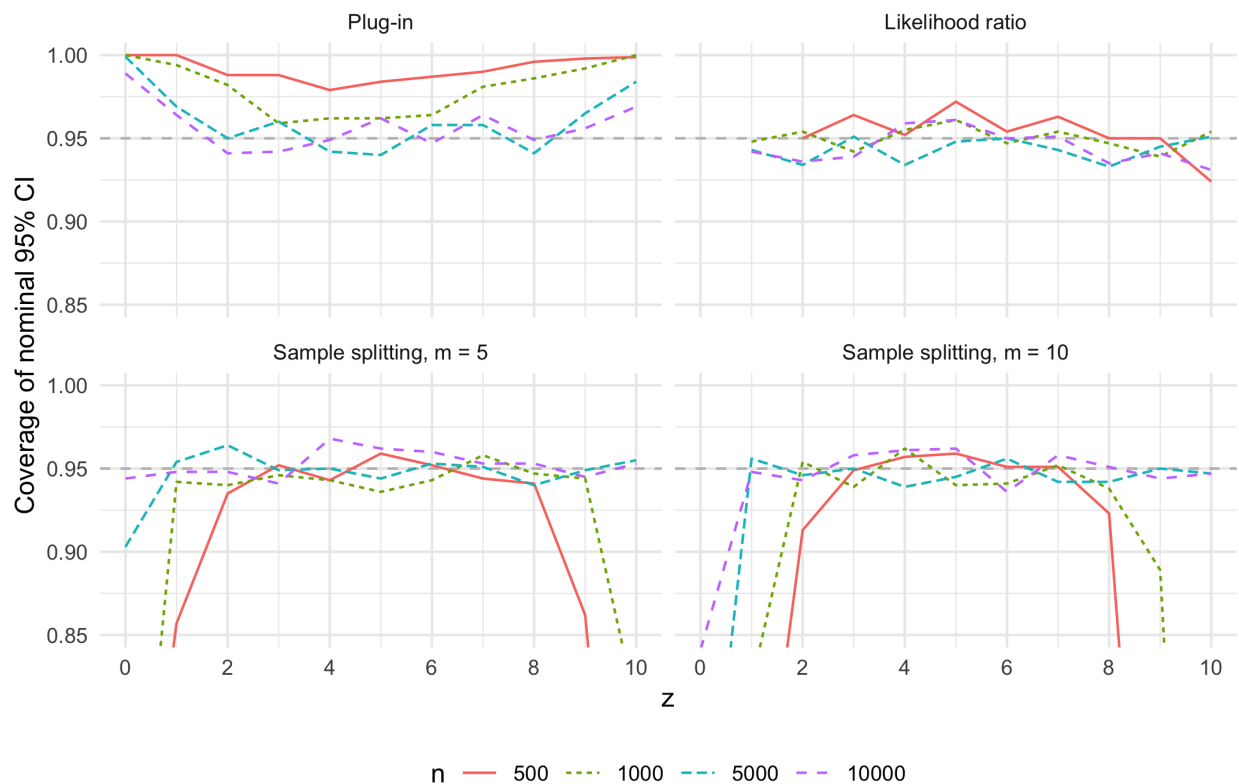


Figure 8: Coverage of 95% CIs in the fully discrete case for $z \in \{0, 1, \dots, 10\}$, various sample sizes n , and four methods: the plug-in method centered around the log of the maximum likelihood estimator (upper left), the inverted likelihood ratio tests (upper right), and the sample splitting method with $m = 5$ (lower left) and $m = 10$ (lower right). Note that the likelihood ratio method does not provide intervals at the endpoints.

Additional simulations: continuous case

We now present results from a numerical study of the properties of the maximum likelihood estimator in the case where both F_0 and G_0 are fully continuous. We set F_0 and G_0 as the distribution functions of exponential random variables with rates 1 and 2, respectively, and we set π_0 to 0.4. We simulated 1000 datasets each for $n \in \{500, 1000, 5000, 10000\}$ and estimated the maximum likelihood estimator, the maximum smoothed likelihood estimator of Yu et al. (2017), the non-monotone estimator based on kernel density estimates for each $z \in \{0, 0.1, \dots, 1.9, 2\}$, and the sample splitting estimator with $m \in \{5, 10, 20\}$ (Banerjee et al., 2019). We constructed confidence intervals at each z using the transformed plug-in and likelihood ratio-based methods described in Section 4.2 of the main text.

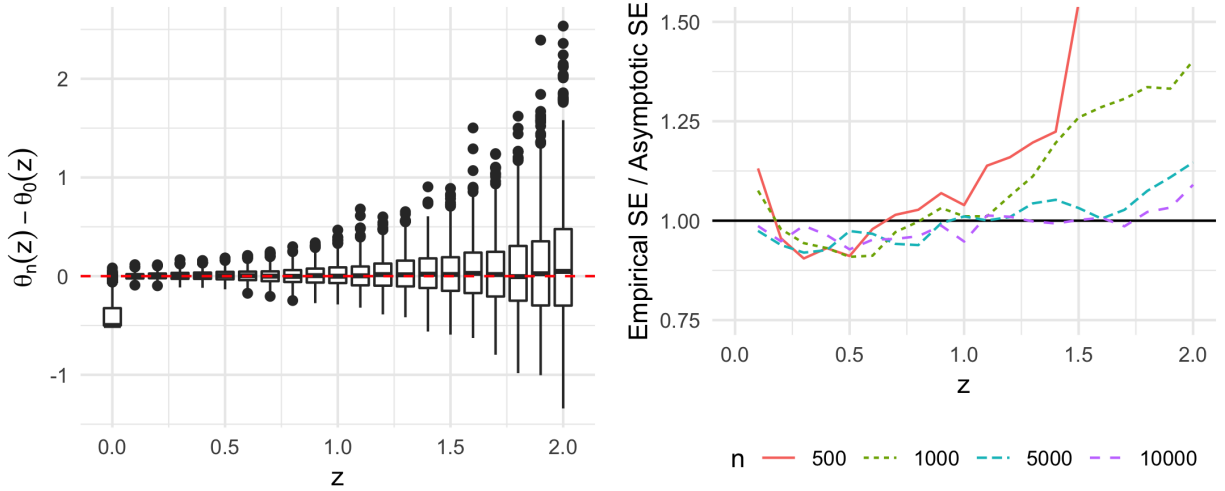


Figure 9: Left: boxplots of $\theta_n^*(z) - \theta_0(z)$ with $n = 10K$ in the fully continuous case. Right: empirical standard errors of $n^{1/2}[\theta_n^*(z) - \theta_0(z)]$ divided by the limit theory-based counterparts for $z \in [0, 2]$.

The left panel of Figure 9 displays the distribution of $\theta_n^*(z) - \theta_0(z)$ for $z \in [0, 2]$, and demonstrates that the sampling distribution of θ_n^* is approximately centered around $\theta_0(z)$ in large samples for $z > 0$. The right panel of Figure 9 displays the ratio of the empirical standard deviation of $n^{1/2}[\theta_n^*(z) - \theta_0(z)]$ to the standard deviation based on the asymptotic theory, and demonstrates that the empirical standard deviation of $\theta_n^*(z)$ approaches the standard deviation defined by the limit theory as the sample size grows.

Figure 10 displays the ratio of the mean squared errors of maximum smoothed likelihood estimator, the kernel density estimator, and the sample splitting estimators to the maximum likelihood estimator. The maximum smoothed likelihood estimator is more efficient than the maximum likelihood estimator. The kernel density estimator is more efficient for some values of z , but less efficient for others. In large enough samples, the sample splitting estimators are more efficient than the maximum likelihood estimator, but in smaller samples, they are less efficient for some values of z . The sample size required for improvement grows with m , as does the gain in asymptotic efficiency.

Finally, Figure 8 shows the empirical coverage of 95% confidence intervals for $\theta_0(z)$ constructed using Wald-type confidence intervals with a plug-in standard error according to the results presented in Section 4.2 of the main text, the inverted likelihood ratio test approach of Banerjee and Wellner (2001), and the sample splitting approach of Banerjee et al. (2019) described in the main text. The plug-in method is conservative in large enough samples due to the difficulty of accurately

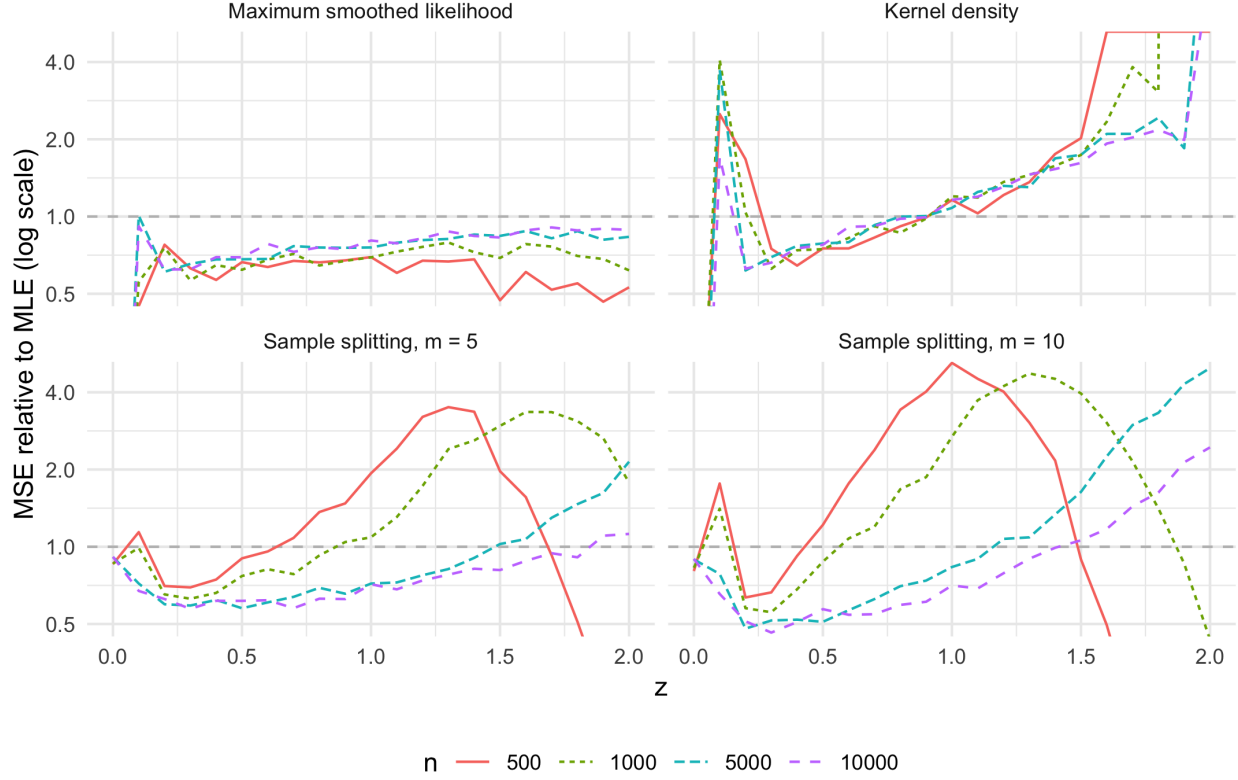


Figure 10: Relative mean squared errors of the maximum smoothed likelihood estimator, the kernel density estimator, and the sample splitting estimators to the maximum likelihood estimator for $z \in [0, 2]$ and various sample sizes n in the fully continuous case. The maximum likelihood has better mean squared error for y -values greater than one, and the other estimator has better mean squared error for y -values less than one.

estimating the derivative of θ_0 . The likelihood ratio method provides slightly conservative coverage at all sample sizes. The sample splitting method has excellent coverage for $m = 5$, but requires larger samples to have good coverage for $m = 10$.

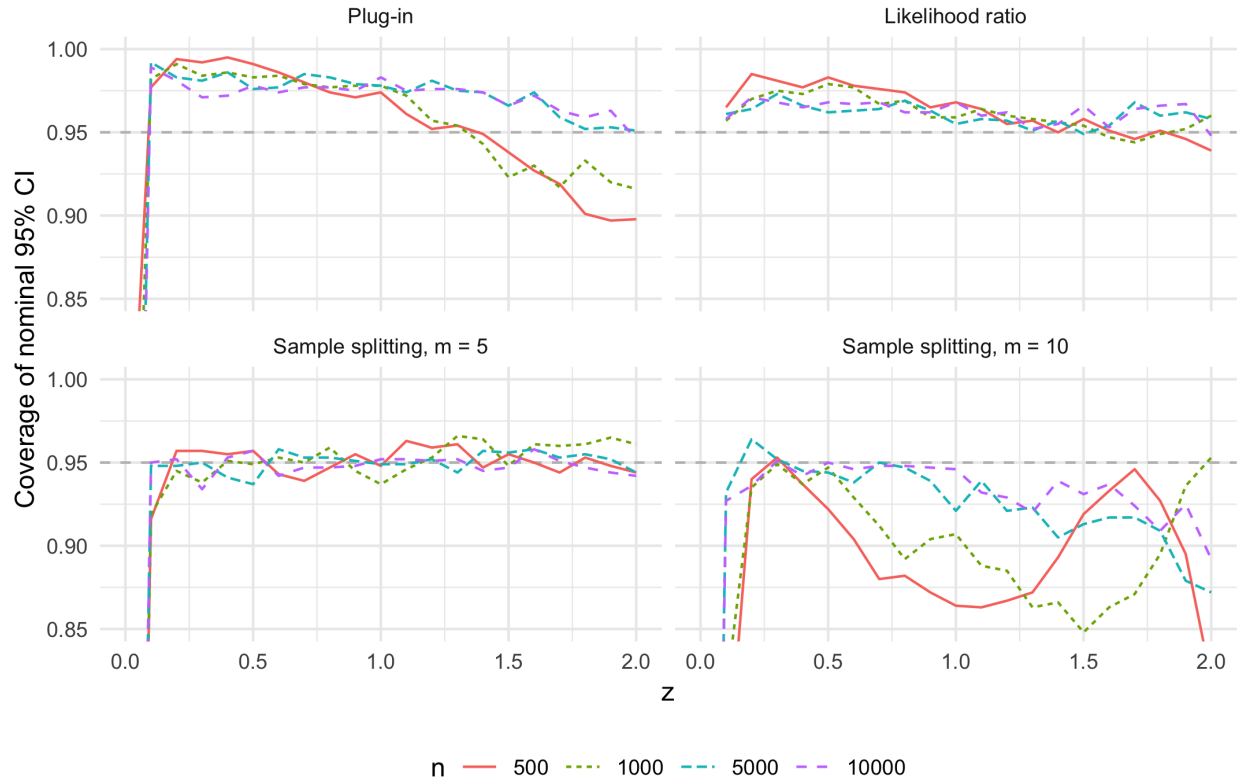


Figure 11: Coverage of 95% CIs in the fully continuous case for $z \in (0, 2]$, various sample sizes n , and four methods: the plug-in method (upper left), the inverted likelihood ratio tests (upper right), and the sample splitting method with $m = 5$ (lower left) and $m = 10$ (lower right).

Additional data analysis results

Figure 12 displays the empirical and likelihood ratio order maximum likelihood cumulative distribution function estimates of C-reactive protein for patients with bacterial infections and those without. Figure 13 displays the empirical and likelihood ratio order maximum likelihood ordinal dominance curve estimates for C-reactive protein.

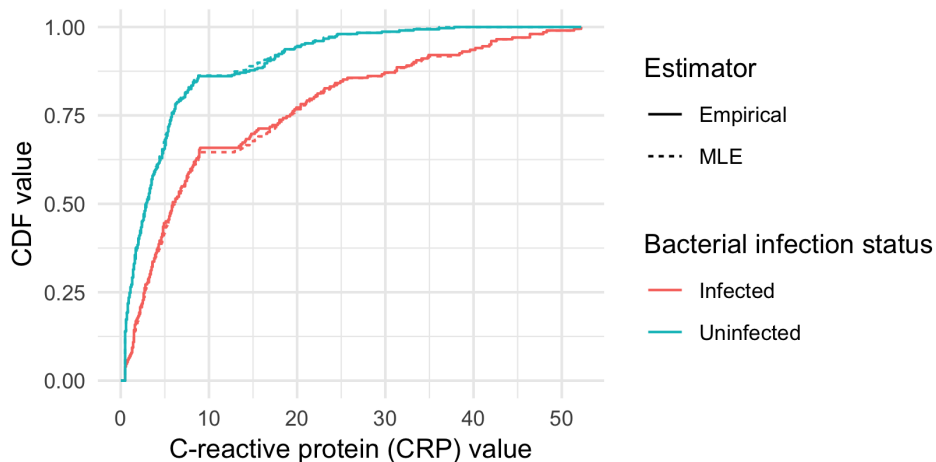


Figure 12: Estimated cumulative distribution functions of C-reactive protein value among patients with bacterial infections and those without. Both the empirical distribution functions and the maximum likelihood estimators under the likelihood ratio order are shown.

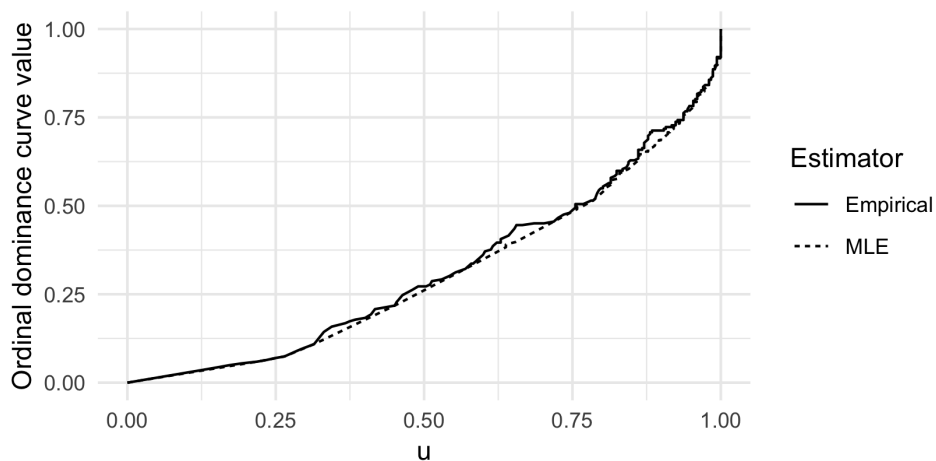


Figure 13: Estimated ordinal dominance curve for C-reactive protein. Both the empirical distribution functions and the maximum likelihood estimators under the likelihood ratio order are shown.